Deep–Sea Research II 227 (2026) 105644

Contents lists available at ScienceDirect

Deep-Sea Research Part II

journal homepage: www.elsevier.com/locate/dsr2

Trophic connections between *Calanus* spp. and deep-sea benthos in the Fram Strait, Arctic Ocean

Dewi Ford [a,*], Katrin Linse [b], Sabena Jane Blackbird [c], Anna K. Wadsworth [a], Jennifer J. Freer [b], Rachel Jeffreys [c], Lydia Anastasia Schmidt [d], Daniel J. Mayor [a]

[a] Biosciences, Hatherly Building, University of Exeter, Exeter, EX4 4PS, United Kingdom
[b] British Antarctic Survey, High Cross, Madingley Road, Cambridge, CB3 0ET, United Kingdom
[c] School of Environmental Sciences, University of Liverpool, Liverpool, L69 3GP, United Kingdom
[d] Institute of Biological Science, University of Rostock, Albert-Einsteinstraße 3, 18059, Rostock, Germany

ARTICLE INFO

Keywords:
Arctic
Biological carbon pump
Biomarker
Copepod
Lipid
Trophic structure

ABSTRACT

Copepods of the genus *Calanus* are central to the ecological and biogeochemical functioning of polar pelagic ecosystems. They graze on seasonal phytoplankton blooms, collectively releasing large quantities of fast-sinking faecal pellets as they convert ingested food into carbon-rich lipid reserves. Towards the end of summer, they migrate down to bathyal and abyssal depths and overwinter by subsisting on their lipid reserves until the following spring. This ontogenetic vertical migration, the so-called 'seasonal lipid pump' (SLP), actively transports enormous quantities of organic matter and surface-derived carbon into the deep ocean. Quantification of the SLP's contribution to the global carbon cycle has attracted major interest, yet little is known about trophic connections between *Calanus* spp. and deep-sea benthic ecosystems. We address this knowledge gap by undertaking lipid biomarker analysis and determining $\delta^{15}N$ signatures of *Calanus* spp. and selected benthic taxa collected from 1255 to 5414 m in the Fram Strait, Arctic Ocean. *Calanus* spp. lipid profiles were dominated by C20:1 and C22:1 fatty acids and alcohols. Substantial quantities of these biomarkers were present in the lipids of all the benthic taxa examined: mean relative abundances ranged from 11.18 mol% in holothurians (trophic level = 1.73) to 29.27 mol% in mysids (trophic level = 2.85). These results suggest an important trophic connection between *Calanus* spp. and deep-sea benthic Arctic ecosystems. We discuss the likely routes through which individual taxa obtain these biomarkers and highlight the potential significance of this trophic link as a pathway for the transferral of organic matter into the deep-sea.

1. Introduction

Copepods within the genus *Calanus* dominate the biomass of mesozooplankton communities in Arctic pelagic ecosystems and play integral roles in the ecological and biogeochemical functioning therein. They represent a critical trophic interface between phytoplankton and higher trophic levels, providing sustenance to a range of fish, birds and marine mammals in the upper ocean (Karnovsky et al., 2003; Varpe et al., 2005; Fortune et al., 2020). Their carbon-rich faecal pellets and exuviae can seasonally dominate the vertical flux of particulate organic matter (e.g., Bathmann et al., 1987), representing an important contribution to the biological gravitational pump. *Calanus* also directly inject carbon into the deep ocean through their ontogenetic vertical migration in a process known as the 'seasonal lipid pump' (SLP; Jónasdóttir et al., 2015). This begins during spring as *Calanus* convert ingested phytoplankton into carbon-rich lipids, predominantly as wax esters, which can almost completely fill an individual's body cavity (Fig. 1). Upon filling their lipid sacs, *Calanus* typically descend to depths >500 m to overwinter in a state of reduced physical and metabolic activity called diapause (Heath et al., 2008; Falk-Petersen et al., 2009; Baumgartner and Tarrant, 2017), thereby transferring surface-derived carbon into the deep ocean.

Carbon released from the respiration of lipids at depth may remain sequestered from the atmosphere for 100's of years (Boyd et al., 2019). A recent estimate suggested that the seasonal vertical migration of just two species of *Calanus*, *C. finmarchicus* and *C. hyperboreus*, inject between 13.6 and 35.8 Gg C yr^{-1} into the deep waters of the Atlantic and Arctic

This article is part of a special issue entitled: LTER HAUSGARTEN published in Deep-Sea Research Part II.

* Corresponding author.
E-mail address: d.ford2@exeter.ac.uk (D. Ford).

https://doi.org/10.1016/j.dsr2.2026.105644
Received 27 June 2025; Received in revised form 23 March 2026; Accepted 30 March 2026
Available online 31 March 2026

Fig. 1. The marine copepod, *Calanus finmarchicus*, with its body cavity almost completely full of lipid. This specimen was collected in the Fram Strait during August 2019 (originally published in Mayor et al., 2020a). Scale bar represents ~1 mm.

Oceans (see Table 3 in Pinti et al., 2023). The realisation that the *Calanus* spp. SLP exports a similar quantity of carbon to the biological gravitational pump (Jónasdóttir et al., 2015; Anderson et al., 2022), coupled with the centennial length-scale of gross sequestration (Boyd et al., 2019), have stimulated a wave of studies to better quantify and understand the SLP in the context of global climate change (Visser et al., 2017; Jónasdóttir et al., 2019; Anderson et al., 2022, 2024; Mayor et al., 2022; Tarling et al., 2022a; Pinti et al., 2023).

Estimating how much carbon the SLP injects into the deep ocean depends in part upon overwintering mortality rates (Visser et al., 2017); copepods may return to the surface ocean with half of their lipid reserves intact (Anderson et al., 2022 and references therein), whereas 100% of the carbon within animals that die during diapause (e.g., via starvation) is assumed to be remineralisation at depth by bacteria (Visser et al., 2017; Tarling et al., 2022a; Pinti et al., 2023). However, if diapausing *Calanus* spp. and/or their carcasses are consumed by non-migratory deep-sea animals, then a significant portion of exported carbon could be directly transferred into deep-sea food webs. This additional trophic pathway for carbon injection would have potential implications for sequestration estimates and our understanding of food supply within high-latitude deep ocean ecosystems. Existing evidence for trophic interactions between *Calanus* spp. and the benthos comes from relatively shallow shelf regions (typically <300 m; e.g., Graeve et al., 1997; Richoux et al., 2005; Søreide et al., 2013), where they clearly serve as an important food source. High densities of *C. hyperboreous* ~1 m above the seafloor have been reported at depths between 2300 and 2500 m in the Fram Strait, Arctic Ocean (Auel et al., 2003; Hirche et al., 2006), suggesting that at least a fraction of the overwintering populations of *Calanus* may also be accessible to supra- and epi-benthic consumers in the deep-sea. Despite this possibility, our knowledge of the trophic linkages between populations of diapausing *Calanus* spp. and high-latitude deep-sea ecosystems remains in its infancy. This knowledge gap hampers our ability to reliably quantify carbon sequestration via the SLP and understand how climate-driven changes to this important biological phenomenon will affect the broader ecology of bathyal and abyssal ecosystems.

One approach to addressing this uncertainty involves tracing trophic connectivity using lipid biomarkers. This is enabled by the large quantities of 20:1(n-9) and 22:1(n-11) fatty acids and alcohols found in *Calanus* spp. wax ester reserves (Hagen et al., 1993; Scott et al., 2002). Unlike most other animals, *Calanus* spp. biosynthesise these specific moieties *de novo* from dietary precursors (Dalsgaard et al., 2003; Sargent and Falk-Petersen, 1988), making it possible to ascribe the presence of these compounds in the tissues of other animals to the consumption of *Calanus* spp.-derived organic matter (Laakmann et al., 2009; Connelly et al., 2014; Parzanini et al., 2018; Maar et al., 2023; Savineau et al., 2024). In addition to lipid biomarkers, nitrogen stable isotope values ($\delta^{15}N$) increase in a predictable, stepwise manner (~3–4 ‰) with each trophic level (Hannides et al., 2009; Duineveld et al., 2012; Connelly et al., 2014). The isotopic signatures of animal tissue can therefore help distinguish carnivores from primary consumers that are less likely to be feeding directly on *Calanus* spp.

This study used $\delta^{15}N$ signatures and the relative abundances of *Calanus* spp. lipid biomarkers to investigate potential trophic connections between *Calanus* spp. and deep-sea (1255–5414 m) benthic invertebrates in the Fram Strait, Arctic Ocean. The purpose of this work was to assess whether *Calanus* spp. support the functioning of the deep-sea food-web in the Fram Strait, and to examine *Calanus*-benthic trophic interactions as a pathway for the vertical transfer of organic matter.

2. Material and methods

2.1. Study region

The long-term ecological research (LTER) observatory HAUSGARTEN is located in the Fram Strait between Greenland and Svalbard (Fig. 2). The west-easterly transect at ~79 °N runs from the eastern Greenland continental shelf towards the Molloy Deep, along the Vestnesa Ridge and onto the Svalbard continental shelf. The northerly transect runs towards the summer sea ice edge. The region is influenced by a highly productive marginal ice zone and is the only deep-water connection between the Nordic Seas and the Arctic Ocean (Soltwedel et al., 2016). On the western side, the Fram Strait is influenced by the cold, less-saline Eastern Greenland Current, while the eastern Fram Strait (EFS, which encompasses most of our stations; Fig. 2) is influenced by the warmer West Spitsbergen Current (Soltwedel et al., 2016). The chlorophyll *a* standing stock in the upper 100 m of the EFS is ~44 mg m^{-2} during the productive season (Nöthig et al., 2015, 2020), though export of particulate organic matter below 300 m is low (<10 %; Bauerfeind et al., 2009).

Zooplankton biomass in the Fram Strait is dominated by the *Calanus* species *C. finmarchicus* and *C. hyperboreus* (Hop et al., 2006; Nöthig et al.,

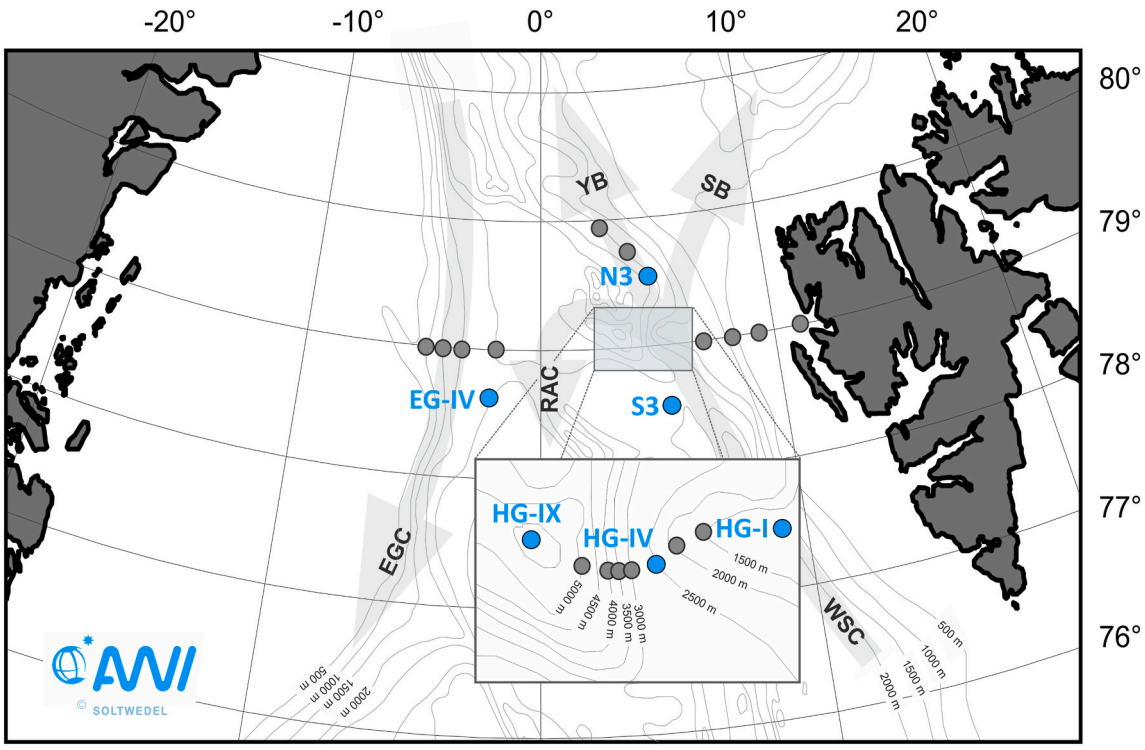

Fig. 2. Map of study area LTER Observatory HAUSGARTEN and Epibenthic Sledge (EBS) stations. Black circles = HAUSGARTEN stations; Red circles = EBS stations; EGC = East Greenland current; RAC = Returen Atlantic Current; SB = Svalbard Branch; WSC = West Spitzbergen Current, YB = Yermack Branch. Map Source: DEIMS iD https://deims.org/f6d9ed12-6bc1-47fb-8e81-ef24e9579596 (Soltwedel, 2025).

2015). *C. finmarchicus* populations are predominantly advected from the sub-Arctic via the West Spitsbergen Current and late copepodite densities are ~16 ind m^3 in upper 1000 m of the EFS during summer (Nöthig et al., 2015; Tarling et al., 2022a). *C. hyperboreus* is a larger, true-Arctic species that is less abundant in the EFS, with densities ranging from ~ 1 to 3 ind m^3 (Auel et al., 2003; Nöthig et al., 2015). Both species are predominantly found in surface waters during the spring/summer (e.g., Kvile et al., 2019; Tarling et al., 2022b), but *C. hyperboreus* is thought to overwinter for longer periods and at deeper depths compared to *C. finmarchicus* (Auel et al., 2003; Kvile et al., 2019).

2.2. Net deployments and sample treatment

C. finmarchicus and *C. hyperboreus* were collected using a BONGO net and a Multi-net. The BONGO net was deployed vertically between 0 and 50 m water depth at HAUSGARTEN site HG-IX (Tables 1 and 2). A Multi-net midi (Hydrobios, Kiel Germany), equipped with five nets of 150 µm mesh size, was towed vertically at HAUSGARTEN sites S3, HG-IV, and N4 to sample five depths layers (1500–1000 m, 999–500 m, 499–200 m, 199–50 m, 49–0 m). The sampled copepods were investigated under a stereomicroscope for species and copepodite stage identification. Where present, batches of 1–5 specimens of each species were picked into cryovials and stored at −80 °C for subsequent lipid analysis. The stage of *Calanus* spp. specimens used for lipid analyses range from CIV to CVI (adult) copepodites (Tables S1 and S2).

2.3. Epibenthic sledge deployments and sample treatment

Supra- and epi-benthic fauna were sampled using a double Epibenthic Sledge (EBS) that followed the design described in Brenke (2005), featuring a bottom shovel that only opened the sampler box doors when the sledge was on the seafloor. The EBS was deployed and towed along the seafloor for 50 min with a varying speed of 0.4–1 knots, depending on sea and ice conditions. The trawl lengths while the EBS was on the seafloor were calculated using the following formula:

$$S = (V1 \times T1) + (V2 \times T2) + (V3 \times T2)$$

Where S = trawl length, T1 = vessel trawling time (min), T2 = cable hauling time until the EBS leaves the seafloor (min), V1 = vessel velocity during trawling (m s^{-1}), V2 = vessel velocity during hauling (until off seafloor; m s^{-1}), V3 = winch velocity while hauling (until off seafloor; m

Table 1
Station data for Multi-net (MN), BONGO (BN), and Epibenthic Sledge (EBS) deployments during sample collections.

Area	Station	Gear	Date	Latitude (start)	Longitude (start)	Water depth (m)	Trawl length (m)
S3	4-6	MN	29/05/2023	78° 36.594′ N	005° 04.049′ E	2325	-
S3	4-11	EBS	29/05/2023	78° 36.172′ N	005° 08.807′ E	2336	1515
HG-IV	5-6	MN	30/05/2023	79° 04.493′ N	004° 14.433′ E	2383	-
HG-IV	5-9	EBS	30/05/2023	79° 04.459′ N	004° 15.343′ E	2372	1011
HG-I	11-14	EBS	03/06/2023	79° 07.336′ N	006° 08.619′ E	1255	795
N3	17-4	MN	05/06/2023	79° 36.259′ N	005° 04.144′ E	2837	-
N3	19-1	EBS	06/06/2023	79° 36.889′ N	005° 19.684′ E	2560	384
HG-IX	27-7	BN	09/06/2023	79° 07.486′ N	002°57.141′ E	5519	-
HG-IX	27-12	EBS	10/06/2023	79° 07.457′ N	002° 45.057′ E	5409	1042
EG IV	30-10	EBS	11/06/2023	78° 36.467′ N	002° 46.748′ W	2545	1861

Table 2
List of benthic invertebrate and *Calanus* copepod samples that were collected from different stations in the Fram Strait for lipid (L) and bulk stable isotope (BSI) analyses. Each copepod L sample consisted of 1 - 5 individuals that were pooled to obtain sufficient biomass for analyses. The first column displays the unique area code and the gear used to collect samples (MN = Multi-net, BN = BONGO, EBS = Epibenthic Sledge), in addition to the start and end depth of the sampling event. The sample number values represent 'n (L)/n (BSI)' for benthic samples and 'n (L)' for copepod samples. Poly. = Polychaeta; Amph. = Amphipoda; Deca. = Decapoda; Isop. = Isopoda; Mysi. = Mysidacea; Holo. = Holothuroidea; Ophi = Ophiuroidea; Chae. = Chaetognatha; *C. fin.* = *Calanus finmarchicus*; *C. hyp.* = *Calanus hyperboreus*.

Area/Gear (start-end)	Poly.	Amph.	Deca.	Isop.	Mysi.	Holo.	Ophi.	Chae.	*C. fin.*	*C. hyp.*
HG-IV/MN (50–0 m)	-	-	-	-	-	-	-	-	3	3
N3/MN (50–0 m)	-	-	-	-	-	-	-	-	1	3
HG-IX/BN (50–0 m)	-	-	-	-	-	-	-	-	2	2
S3/MN (200–40 m)	-	-	-	-	-	-	-	-	2	-
HG-IV/MN (200–50 m)	-	-	-	-	-	-	-	-	3	2
S3/MN (500–200 m)	-	-	-	-	-	-	-	-	-	3
S3/MN (1000–500 m)	-	-	-	-	-	-	-	-	-	3
HG-I/EBS (1255–1254 m)	1/1	5/8	-	2/2	-	-	5/7	1/0	1	-
S3/EBS (2336–2328 m)	-	6/9	2/3	-	2/4	2/4	-	1/0	-	-
HG-IV/EBS (2372–2382 m)	-	2/3	2/3	-	1/2	-	-	-	-	2
EG-IV/EBS (2545–2551 m)	-	1/3	-	1/1	5/7	2/3	-	-	-	-
N3/EBS (2560–2587 m)	1/2	1/1	1/1	-	-	2/3	-	1/0	-	1
HG-IX/EBS (5409–5414 m)	1/2	3/4	-	-	-	6/9	-	-	-	-

s^{-1}). Upon arrival on deck, the cod ends were retrieved from the nets and immediately transported to the cooling container (4 °C). Here, cod end samples were sieved in pre-cooled filtered seawater over a 300 μm mesh. Floating crustaceans were removed with a 300 μm mesh sieve to check for *C. finmarchicus* and *C. hyperboreus*. When available, net supernatant was sieved on deck at the sieving table with filtered seawater over stacked 1000 μm, 500 μm, and 300 μm sieves. Invertebrates visible to the eye were removed from the sieves for photographing and subsequent fixing for morphological identification, lipid analyses, and stable isotope analyses. When three or more specimens per morphospecies were present, one specimen was photographed and at least one specimen per morphospecies fixed in undenatured 96 % ethanol, RNA-later, or frozen at −80 °C. All specimens used for lipid and stable isotope analyses were frozen at −80 °C in cryovials. Macrozoobenthic specimens were frozen as singletons, while *C. finmarchicus* and *C. hyperboreus* were checked for their copepodite stage and frozen in batches of 1–5 specimens per copepodite stage as per previous methods. Invertebrate taxa collected by the EBS (excluding *Calanus* spp.) are addressed as "benthic" from here on.

Specimens of representative macro-and megafauna were photographed with a digital Canon EOS 5D Mark IV SLR camera, using a mounted macro-objective MP-E65mm f/2.8 1–5x for the macrofauna and an EF50mm f/2.5 Compact objective for the megafauna, and two linked flashes on a Kaiser RS copy stand.

2.4. Laboratory lipid sample treatment and gas chromatograph analyses

Lipid extractions were carried out on each homogenized freeze-dried (−60 °C; 10^{-2} mBar) sample (0.3–100 mg dry weight). A known quantity of an internal standard (1–20 μgL of 5 α (H)-cholestane) was

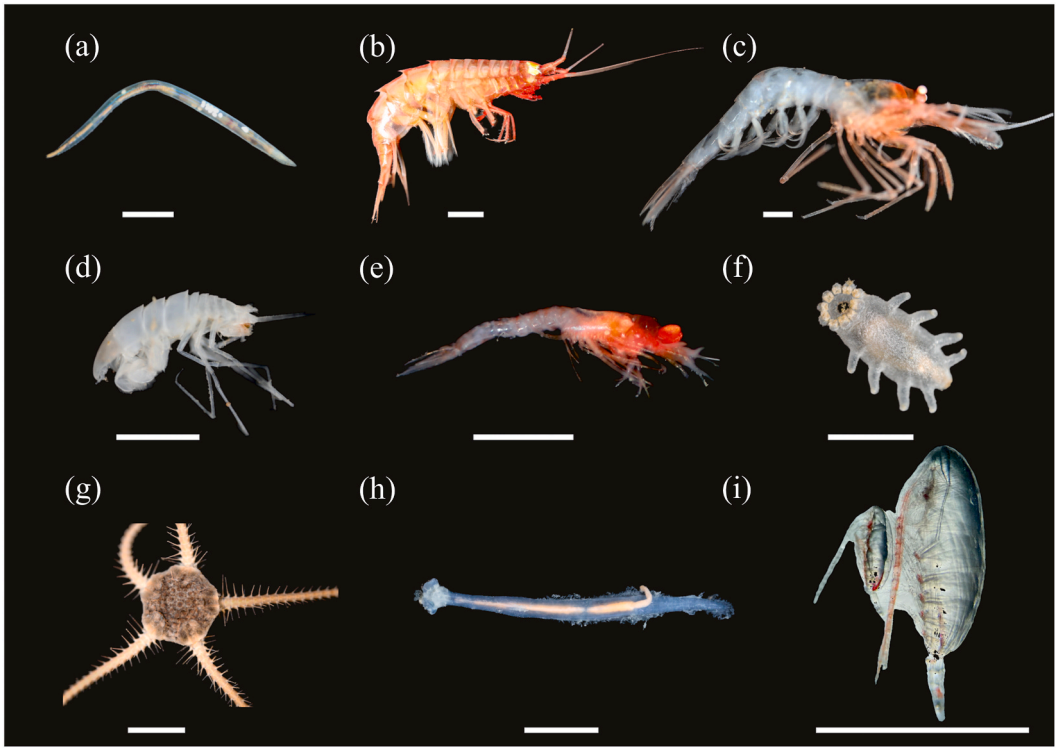

Fig. 3. Representatives of the analysed taxa. (a) Polychaeta, (b) Amphipoda, (c) Decapoda, (d) Isopoda, (e) Mysidacea, (f) Holothuroidea, (g) Ophiuroidea, (h) Chaetognatha, (i; left) *Calanus finmarchicus*, (i; right) *Calanus hyperboreus*. Scale bars = 5 mm.

added to each sample, followed by a mixture of dichloromethane (DCM) and methanol (9:1; 25 mL). The samples were then sonicated (15 min, twice) and the resulting extract was decanted into round bottom flasks. The solvent obtained was evaporated to dryness under vacuum using a rotary evaporator at ~30 °C. Each sample was then passed through a Pasteur pipette filled with anhydrous sodium sulphate using DCM (3 mL).

The solvent was blown down with nitrogen gas and the samples were stored (−20 °C) before transmethylation (10 % acetyl chloride/methanol), passed through a Pasteur pipette filled with anhydrous potassium carbonate using DCM (3 mL) and blown down under nitrogen gas to dryness. The samples were finally derivatised with N,O-Bis (trimethylsilyl)trifluoroacetamide (BSTFA; 60 μL, 40 °C, 45 min), blown down under nitrogen gas, and stored at −20 °C until analysis.

Gas chromatography-mass spectrometry (GC-MS) analyses of the total lipid extracts were conducted using a GC Trace 1300 fitted with a split-splitless injector and column DB-5MS (60m × 0.25 mm) featuring a film thickness of 0.1 μm, non-polar stationary phase of 5 % phenyl and 95 % methyl silicone, and using helium as a carrier gas (2 mL min^{-1}). The GC oven was programmed after 1 min from 60 °C to 170 °C at 6 °C min^{-1}, then from 170 °C to 315 °C at 2.5 °C min^{-1} and held at 315 °C for 15 min. The eluent from the GC was transferred directly via a transfer line (320 °C) to the electron impact source of a Thermoquest ISQMS single quadrupole mass spectrometer. Typical operating conditions were as follows: ionisation potential = 70 eV; source temperature = 215 °C; trap current = 300 μA. Mass data were collected at a resolution of 600 Da, cycling every second from 50 to 600 Da and were processed using Xcalibur software. Compounds were identified either by comparison of their mass spectra and relative retention indices with those available in the literature, and/or by comparison with authentic standards. Shorthand notations of fatty acids and alcohols follow the IUPAC (International Union of Pure and Applied Chemistry, hhttp://www.iupac.org) systematic nomenclature 'n-x' notation. Quantitative data were calculated by comparison of peak areas of the internal standard with those of the compounds of interest, using the total ion current (TIC) chromatogram. The relative response factors of the analytes were determined individually for 36 representative fatty acids and sterols using authentic standards. Response factors for analytes where standards were unavailable were assumed to be identical to those of available compounds of the same class.

2.5. Laboratory bulk stable isotope sample treatment

Samples were defatted by a mixture of dichloromethane (DCM) and methanol (9:1; 25 mL). The samples were then sonicated (15 min, twice) and the resulting extract was discarded. Samples were analysed following acid vapour treatment (HCL; 12 h; Yamamuro and Kayanne, 1995), using an ECS8020 elemental analyser (NC Technologies) coupled to a Delta V isotope ratio mass spectrometer (Thermo Scientific). Isotope values were corrected using internationally certified isotopic reference materials USGS40 and USGS41a (Reston Stable Isotope Laboratory) and are reported in δ-notation (‰) relative to atmospheric nitrogen (N_2) and Vienna PeeDee Belemnite carbonate (V-PDB) scales. An internal standard of homogenized prawn (*Penaeus vannamei)* with well characterized $\delta^{15}N$ values (6.50 ± 0.16 ‰) was used to measure precision.

2.6. Data analyses

Higher-level benthic taxa with fewer than three samples were excluded from all analyses. The key taxa selected from this criterion included the crustacean orders Amphipoda, Decapoda, Isopoda, and Mysidacea, the echinoderm classes Holothuroidea and Ophiuroidea, the paraphyletic class Polychaeta, and the phyla Chaetognatha (Fig. 3, Table 2). The specimens from most taxa were comprised of a single morphospecies; exceptions included Mysidacea and Polychaeta, which featured two morphospecies, and Amphipoda, which featured nine (species listed in the Results). Our statistical analyses were therefore focused on differences among higher-level taxa.

Quantitative lipid constituent data were separated into three datasets which included lipid homologous groups (e.g., fatty acids, alcohols, sterols), individual fatty acids, and individual fatty alcohols. These data were converted to relative abundance (mol%) of total identified lipid groups, individual fatty acids, or individual fatty alcohols, respectively. The relative abundance of fatty acid isomers with the same number of carbon molecules and double bounds but unidentified omega groups were summed and labelled as 'X1:X2(iso)'.

Principal Component Analysis (PCA) was conducted on centred and scaled relative abundance data to examine variation in lipid composition among taxa and identify which constituents were associated with *Calanus* spp. (Dixon, 2003). Lipid homologous groups, individual fatty acids, and individual fatty alcohols were analysed independently. To prevent minor lipid constituents from skewing results, constituents with median relative abundances <1 mol% for both benthic and *Calanus* taxa were excluded from all analyses. The relative abundances were then corrected to ensure the sum of all selected constituents within each sample was equal to 100 %. Redundancy Analysis (RDA), an extension of PCA, was subsequently used to determine how much of the variation in lipid composition could be explained by taxa and mean depth (based on sampling start and end depth measurements) (Mayor et al., 2013; Savineau et al., 2024). Significant explanatory terms were identified using a hierarchical backward selection procedure (Mayor et al., 2010, 2013). Initial RDA models included both taxa and depth as explanatory terms; the interaction between both variables could not be incorporated into the model due to collinearity (variance inflation factor values were >5 for multiple taxa-depth interactions). These models were then compared with simplified models by using Analysis of Variance (ANOVA) to determine if removing either explanatory term significantly decreased the model's accuracy.

The relative abundance of known *Calanus* spp. lipid biomarkers (i.e. 20:1 and 22:1 moieties; Hagen et al., 1993; Scott et al., 2002) that were also associated with *Calanus* spp. within our PCA results were then compared among taxa. The selected biomarkers included the fatty acid 20:1(n-9), the sum of the fatty acids 22:1(n-11) and 22:1(iso), and the sum of 20:1 and 22:1 fatty acid and alcohol isomers. Data for the latter were converted to mol% of total fatty acids and alcohols within each sample. The relationship between sample depth and the relative abundance of *Calanus* spp. biomarkers, polyunsaturated fatty acids (PUFA, which are thought to be linked to diapause; Pond, 2012), or the total concentration of lipids (expressed as mg g^{-1} [dry weight]) were examined using linear regression. Separate analyses were conducted for *Calanus* spp. and benthic taxa to avoid lipid differences between these two groups from masking the potential effects of depth.

ANOVA was used to compare the bulk $\delta^{15}N$ signatures of different

benthic taxa. Post-hoc analyses were conducted using Tukey's Honestly Significant Difference (HSD) tests. Bulk $\delta^{15}N$ signatures were also used to calculate estimated trophic levels of our benthic specimens based on the following equation:

$$\text{Trophic Level} = 1 + \frac{\delta^{15}N_{consumer} - \delta^{15}N_{baseline}}{\delta^{15}N_{enrichment}}$$

Where $\delta^{15}N_{consumer}$ represents the $\delta^{15}N$ signature of the sample, $\delta^{15}N_{baseline}$ represents the mean $\delta^{15}N$ signature of bottom sediments from the Fram Strait (4.43 ‰), as previously reported by Bergmann et al. (2009), and $\delta^{15}N_{enrichment}$ represents an enrichment factor of 3.80 ‰ per trophic level in line with previous Arctic food web studies (Bergmann et al., 2009 and references therein). We did not determine $\delta^{15}N$ signatures of *C. finmarchicus* and *C. hyperboreus* tissues, therefore previously published $\delta^{15}N$ values for Arctic specimens (means = 7.18 ± 0.65 ‰ and 7.78 ± 0.86 ‰, respectively; see Table 4 in Søreide et al., 2008) were used to assess whether the isotopic composition of benthic organisms in our study was consistent with the consumption of *Calanus* spp. Benthic organisms that consume *Calanus* spp. would be expected to exhibit enriched $\delta^{15}N$ signatures relative to those of *Calanus* spp. specimens.

3. Results

3.1. Supra-benthic Calanus spp

Most of the *Calanus* spp. used for lipid analyses were collected from plankton net deployments at 0–500 m (Table 2). However, it is noteworthy that both species were also collected during Epibenthic Sledge (EBS) deployments at >1000 m. Adult female *Calanus finmarchicus* were collected at ~1255 m (five individuals pooled into a single sample for lipid analysis; Table 2 and S1). The pooled lipid concentration of these bathyal specimens was 16.52 mg g^{-1} (dry weight), which was markedly less than mean concentration for this species (94.29 ± 64.35; Table 3). *Calanus hyperboreus* (≥CIV copepodites) were collected during two EBS deployments at ~2372 m and 2560 m (Table 2 and S2). Their lipid concentrations were similar (149.19–169.65 mg g^{-1}), but their dry weights ranged from 368.40 μg to 5300 μg (Table S2). Bathyal specimens of both species were sluggish, in good condition, and featured clear bodies, indicating that they were in diapause. *C. hyperboreus* specimens also featured visible but depleted lipid sacs.

3.2. Lipid analyses

Lipid concentrations were highly variable among the analysed taxa (Table 3). Non-crustacean taxa exhibited low mean concentrations; the lowest value was 2.22 ± 1.54 mg g^{-1} (dry weight) in holothurians. By contrast, mean concentrations ranged from 82.39 to 155.78 mg g^{-1} in amphipods, mysids, and *Calanus* spp., with the highest values observed in specimens of *C. hyperboreus*.

The lipid profiles of benthic taxa were dominated by fatty acids (Table 3). Monounsaturated fatty acids (MUFA) were the most abundant homologous group found in all benthic taxa, ranging from 36.39 ± 8.28 mol% in holothurians to 59.53 ± 10.22 mol% in mysids. Most benthic taxa had a similar abundance of saturated fatty acids (SFA) and polyunsaturated fatty acids (PUFA). Exceptions included amphipods and decapods, whereby the relative abundances of PUFA were roughly twofold that of SFA (Table 3). MUFA and PUFA were also abundant in *C. finmarchicus* and *C. hyperboreus*; both copepod species exhibited similar concentrations of MUFA (27.99 ± 14.65 and 26.67 ± 8.11 mol %, respectively) but *C. hyperboreus* featured a lower relative abundance of SFA (5.25 ± 2.18 mol%) and a higher relative abundance of PUFA (26.35 ± 14.88 mol%) compared to *C. finmarchicus*, highlighting a greater degree of fatty acid unsaturation. Unsaturated fatty alcohols (UAL) were the dominant group identified in both *C. finmarchicus* and *C. hyperboreus* (33.09 ± 13.02 mol% and 32.86 ± 9.67 mol%, respectively). In contrast, the lipid profiles of most benthic taxa included <2 mol% UAL, except for chaetognaths (6.45 ± 8.33 mol%). Holothurians featured the highest relative abundance of sterols (22.99 ± 15.09 mol %).

Principal Component Analysis (PCA) results demonstrated that 37 % of the variation in the relative abundances of lipid homologous groups could be explained by PC1 and 21 % could be explained in PC2. Redundancy Analysis (RDA) revealed that this variation was influenced by both taxa ($F_{9,77} = 10.78$, $p < 0.001$) and water depth ($F_{1,77} = 2.47$, $p < 0.05$), which together explained 56.37 % of the variability (Fig. 4). However, variability explained by the RDA only decreased by 1.40 % when depth was excluded, highlighting its minimal explanatory power compared to taxa (and therefore its exclusion from Fig. 4). The data visually partitioned into three different clusters; *Calanus* spp., holothurians, and the other benthic taxa (Fig. 4). The non-holothurian benthic taxa were associated with SFA and MUFA, whereas holothurians featured higher relative abundances of branched fatty acids (BRFA) and sterols. In contrast, the biomarker compositions of *C. finmarchicus* and *C. hyperboreus* were associated with saturated fatty alcohols (SAL) and UAL. The relative abundance of PUFA exhibited limited influence on the overall variation.

18:1(n-9) was the dominant fatty acid across all benthic taxa, ranging from 20.00 ± 1.45 mol% in decapod samples to 36.47 ± 14.81 mol% in polychaetes (Table 4). 16:0, 20:1(n-9), and 20:5(n-3) were also consistently prevalent (each >5 mol%) in the benthic samples (Table 4). *C. finmarchicus* and *C. hyperboreus* exhibited more uniform fatty acid profiles that were not dominated by a single class. *C. finmarchicus* exhibited a high relative abundance of 14:0, 16:0, 18:1(n-9), and 20:1(n-9) (18.08 ± 19.03, 13.49 ± 6.16, 11.32 ± 16.02, and 13.93 ± 5.63 mol %, respectively). *C. hyperboreus* also showed a high relative abundance of 20:1(n-9) (19.04 ± 5.44 mol%), but the second most abundant fatty acid was 22:6(n-3) (11.11 ± 6.50 mol%) and most other fatty acids ranged from approximately 4–8 mol% (Table 4). The fatty alcohol profiles of *C. finmarchicus* and *C. hyperboreus* were largely dominated by 20:1 (34.27 ± 5.59 and 29.24 ± 5.71 mol%, respectively) and 22:1 (44.90 ± 9.26 and 45.99 ± 9.98 mol%, respectively; Table 5). The fatty alcohol composition of the benthos highlighted the prevalence of 16:0, 20:1, and 22:1 across all taxa (Table 5).

PC1 explained 27 % of the variation in the relative abundances of individual fatty acids and PC2 explained 15 %. This variation was influenced by taxa ($F_{9,76} = 7.341$ $p < 0.001$) and water depth ($F_{1,76} = 2.35$, $p < 0.05$), which together explained 47.63 % of the variability (Fig. 5), although removing depth as an explanatory variable only decreased variance explained by 1.62 %. Three clusters were again apparent: *Calanus* spp., holothurians, and the other benthic taxa. The fatty acid profiles of holothurians featured higher relative abundances of 18:0, 20:4(n-6), and branched fatty acids, whereas the other benthic taxa exhibited similar fatty acid compositions and were associated with 18:1(n-9). The fatty acid profiles of *C. finmarchicus* and *C. hyperboreus* were associated with 20:1(n-9), 22:1(n-11) and 22:1(iso).

PC1 explained 32 % of the variation in the relative abundances of

Table 3
Mean ± SD dry weight (DW, mg), total lipid content (TLC, mg g^{-1} dry weight), and relative abundance of different lipid homologous groups (mol% of total lipids) measured in benthic invertebrate and copepod samples. Poly. = Polychaeta; Amph. = Amphipoda; Deca. = Decapoda; Isop. = Isopoda; Mysi. = Mysidacea; Holo. = Holothuroidea; Ophi. = Ophiuroidea; Chae. = Chaetognatha; *C. fin.* = *Calanus finmarchicus*; *C. hyp.* = *Calanus hyperboreus*; SFA = saturated fatty acids; MUFA = monounsaturated fatty acids; PUFA = polyunsaturated fatty acids; BRFA = branched fatty acids; SAL = saturated fatty alcohols; UAL = unsaturated fatty alcohols; ST = sterols. Header text below taxa shows sample depth range (m).

	Poly. 1254–5414	Amph. 1254–5414	Deca. 2328–2587	Isop. 1254–2551	Mysi. 2328–2551	Holo. 2328–5414	Ophi. 1254–1255	Chae. 1254–2587	*C. fin.* 0–1255	*C. hyp.* 0–2587
n	3	18	5	3	8	12	5	3	12	19
DW	0.55 ± 0.43	36.18 ± 37.12	82.76 ± 29.61	2.07 ± 1.76	43.54 ± 15.14	12.54 ± 7.31	10.78 ± 4.00	1.47 ± 0.55	0.15 ± 0.09	2.17 ± 1.39
TLC	39.58 ± 25.33	82.39 ± 85.47	49.34 ± 34.63	61.87 ± 47.96	112.77 ± 62.06	2.22 ± 1.54	19.73 ± 15.57	61.16 ± 49.03	94.29 ± 64.35	155.78 ± 80.83
SFA	13.67 ± 5.94	15.26 ± 3.70	13.89 ± 2.46	20.49 ± 5.06	13.38 ± 3.23	13.02 ± 4.04	18.93 ± 4.81	18.49 ± 4.66	20.40 ± 12.71	5.25 ± 2.18
MUFA	57.19 ± 11.62	50.53 ± 12.96	47.29 ± 4.03	52.69 ± 7.27	59.53 ± 10.22	36.39 ± 8.38	50.05 ± 18.52	53.46 ± 14.58	27.99 ± 14.65	26.67 ± 8.11
PUFA	16.07 ± 1.83	27.65 ± 15.38	31.16 ± 4.93	19.04 ± 4.56	19.14 ± 6.52	20.46 ± 10.39	17.65 ± 6.06	17.22 ± 11.21	12.48 ± 12.30	26.35 ± 14.88
BRFA	1.33 ± 0.57	1.05 ± 0.75	1.89 ± 0.35	1.42 ± 0.54	0.64 ± 0.47	4.92 ± 2.35	2.38 ± 1.10	0.72 ± 0.12	0.83 ± 0.31	0.18 ± 0.12
SAL	1.23 ± 1.07	0.37 ± 0.74	0.49 ± 0.37	0.39 ± 0.47	0.29 ± 0.37	0.94 ± 0.89	0.22 ± 0.14	1.83 ± 1.34	4.37 ± 2.97	8.06 ± 6.22
UAL	0.28 ± 0.49	2.15 ± 6.28	1.71 ± 1.16	0.24 ± 0.42	3.85 ± 4.93	0.35 ± 0.64	1.20 ± 1.32	6.45 ± 7.34	33.02 ± 13.85	32.86 ± 9.67
ST	10.10 ± 5.41	2.97 ± 2.84	3.48 ± 2.26	5.73 ± 4.25	3.16 ± 2.90	22.99 ± 15.09	9.45 ± 7.05	1.83 ± 1.46	0.85 ± 0.72	0.58 ± 0.38

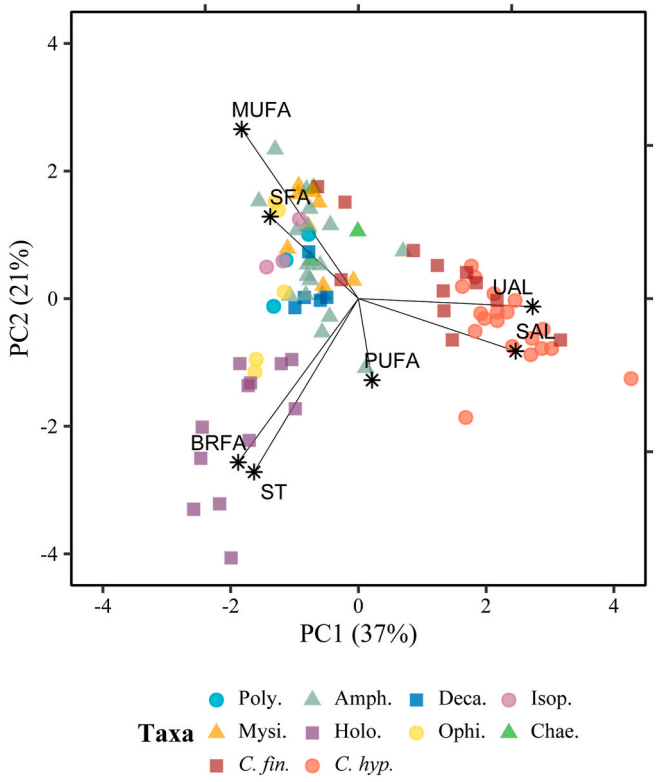

Fig. 4. Principal component analysis plot showing variation in the relative abundance (mol%) of different lipid homologous groups and how lipid compositions differed among taxa (taxa and water depth collectively explained 56.37 % of the variability, taxa accounted for 54.97 %). Points represent individual samples. SFA = saturated fatty acids; MUFA = monounsaturated fatty acids; PUFA = polyunsaturated fatty acids; BRFA = branched fatty acids; SAL = saturated fatty alcohols; UAL = unsaturated fatty alcohols; ST = sterols. Poly. = Polychaeta; Amph. = Amphipoda; Deca. = Decapoda; Isop. = Isopoda; Mysi. = Mysidacea; Holo. = Holothuroidea; Ophi = Ophiuroidea; Chae. = Chaetognatha; *C. fin.* = *Calanus finmarchicus*; *C. hyp.* = *Calanus hyperboreus*.

individual fatty alcohols and PC2 explained 19 %. Taxa accounted for 25.25% of the variability in fatty alcohol composition ($F_{9,76} = 2.85$, $p < 0.001$), whereas including depth as an explanatory variable did not significantly increase how much variance the RDA could explain ($p > 0.05$). The *Calanus* spp., holothurians, and the other benthic taxa clusters remained apparent, although they were less visually discernible than in the lipid and fatty acid analyses (Fig. 6). *Calanus* spp. and most benthic taxa were separated from holothurians on account of their association with 20:1 and 22:1 fatty alcohols (Fig. 6).

3.3. *Calanus* spp. biomarkers

The *Calanus* spp. fatty acid biomarkers 20:1(n-9) and 22:1(n-11 + iso) were detected in all benthic taxa (Table 4; Fig. 7). Chaetognaths (14.33 ± 4.90 mol%), mysids (10.99 ± 2.70 mol%), and ophiuroids (10.73 ± 2.77 mol%) exhibited similar levels of 20:1(n-9) relative to *Calanus* spp., whereas holothurians showed notably lower levels (3.34 ± 2.91 mol%). A different pattern was observed for 22:1(n-11 + iso); chaetognaths (6.86 ± 1.88 mol%), holothurians (4.94 ± 4.20 mol%), decapods (4.47 ± 1.14 mol%), and mysids (4.45 ± 2.41 mol%) exhibited the highest relative abundances of these fatty acids among the benthic taxa (Table 4; Fig. 7).

When combined, 20:1 and 22:1 fatty acids and alcohols accounted for 44.13 ± 12.89 mol% and 49.10 ± 14.43 mol% of the total fatty acid/alcohol pools of *C. finmarchicus* and *C. hyperboreus,* respectively (Fig. 7). These abundances were substantially higher than those observed in benthic specimens. Nevertheless, these compounds were still present in moderate to high levels across all benthic taxa. Mysids (29.27 ± 8.67 mol%), chaetognaths (27.27 ± 10.72 mol%), polychaetes (22.49 ± 5.57 mol%), and decapods (21.28 ± 4.01 mol%) exhibited the highest relative abundances among benthic taxa, while holothurians (11.18 ± 5.22 mol%), isopods (13.18 ± 10.45 mol%), and amphipods (15.22 ± 10.39 mol%) exhibited the lowest. Ophiuroids (18.15 ± 4.81 mol%) displayed intermediate levels.

There were no clear species-specific differences in the relative abundance of total *Calanus* spp. biomarkers (20:1 and 22:1 fatty acids and alcohols) between the two Mysidacea and Polychaeta morphospecies identified (Table 6). Conversely, distinct levels of *Calanus* spp. biomarkers were apparent among the nine morphospecies of Amphipoda identified (Table 6). The mean relative abundances of *Calanus* spp. biomarkers were lowest in *Cyphocaris* cf. *bouvieri* (4.40 ± 3.17 mol%) and *Halirages spongiae* (9.15 ± 4.13 mol%) but ranged from 20.28 to 39.55 mol% in *Anonyx nugax*, *Eurythenes* sp., and Stegocephalidae (family) sp. (one sample per species). Table 6 also shows the concentrations of *Calanus* spp. lipid biomarkers per individual or dry weight. Of the benthic taxa analysed, the mean concentrations of total *Calanus* spp. biomarkers were highest in mysids (38.03 ± 26.56 mg g^{-1}), but the highest individual concentration was found in an amphipod (*Anonyx nugax*) specimen collected at ~5409 m (85.14 mg g^{-1}). Mean concentrations were particularly low in holothurians (0.17 ± 0.15 mg g^{-1}) and ophiuroids (3.95 ± 3.93 mg g^{-1}), owing to their reduced total lipid concentrations (Table 6).

Table 4
Mean ± SD relative abundance (mol% of total fatty acids) of key fatty acid groups identified in benthic invertebrate and copepod samples. Fatty acid groups with median relative abundances of <1 % in either benthic or copepod samples have been excluded. Poly. = Polychaeta; Amph. = Amphipoda; Deca. = Decapoda; Isop. = Isopoda; Mysi. = Mysidacea; Holo. = Holothuroidea; Ophi. = Ophiuroidea; Chae. = Chaetognatha; *C. fin.* = *Calanus finmarchicus*; *C. hyp.* = *Calanus hyperboreus*; X:Y (iso) = total relative abundance of X:Y isomers with unidentified omega groups. Header text below taxa shows sample depth range (m).

	Poly. 1254–5414	Amph. 1254–5414	Deca. 2328–2587	Isop. 1254–2551	Mysi. 2328–2551	Holo. 2328–5414	Ophi. 1254–1255	Chae. 1254–2587	*C. fin.* 0–1255	*C. hyp.* 0–2587
n	3	18	5	3	8	12	5	3	12	18
14:0	0.65 ± 0.34	2.01 ± 1.10	2.50 ± 2.10	2.69 ± 0.18	2.19 ± 0.89	1.29 ± 0.85	4.31 ± 1.56	3.62 ± 4.93	18.08 ± 19.03	4.16 ± 1.35
16:0	10.92 ± 5.41	12.48 ± 3.79	9.43 ± 1.32	16.63 ± 4.82	10.89 ± 3.09	9.31 ± 2.92	12.12 ± 3.87	15.26 ± 2.56	13.49 ± 6.16	4.33 ± 2.20
18:0	2.82 ± 1.96	0.81 ± 0.54	1.28 ± 0.23	1.63 ± 1.06	0.37 ± 0.23	3.44 ± 1.32	3.26 ± 1.87	1.43 ± 0.60	1.04 ± 0.92	0.54 ± 0.28
16:1(n-7)	1.21 ± 2.10	6.13 ± 3.02	5.06 ± 4.65	12.47 ± 4.66	5.00 ± 1.60	9.71 ± 6.43	3.16 ± 3.52	7.02 ± 3.82	5.76 ± 3.16	3.14 ± 3.10
18:1(n-9)	36.47 ± 14.81	30.87 ± 13.49	20.00 ± 1.45	28.26 ± 0.24	29.74 ± 5.82	20.01 ± 6.19	29.35 ± 17.31	23.83 ± 13.66	11.32 ± 16.01	7.87 ± 7.10
20:1(n-9)	8.50 ± 4.69	7.73 ± 4.66	7.35 ± 1.90	7.30 ± 5.54	10.99 ± 3.00	3.34 ± 2.91	10.73 ± 2.77	14.33 ± 4.90	13.93 ± 5.63	19.04 ± 5.44
20:1(iso)	12.11 ± 5.70	3.58 ± 2.61	8.44 ± 3.82	2.28 ± 1.37	11.53 ± 6.34	2.80 ± 1.39	3.39 ± 1.22	3.13 ± 1.54	1.55 ± 0.53	3.31 ± 1.12
22:1(n-11)	0.59 ± 0.79	0.91 ± 1.29	2.21 ± 1.35	0.57 ± 0.37	1.18 ± 0.97	1.67 ± 4.38	0.58 ± 0.42	1.06 ± 0.07	5.14 ± 4.56	4.88 ± 3.72
22:1(iso)	1.34 ± 1.93	2.00 ± 1.89	2.25 ± 0.46	2.88 ± 2.87	3.27 ± 2.41	3.27 ± 2.22	2.88 ± 2.01	5.79 ± 1.82	3.77 ± 3.75	5.92 ± 3.29
20:4(n-6)	1.09 ± 0.50	1.86 ± 1.43	2.32 ± 1.10	1.98 ± 0.47	1.20 ± 0.88	7.15 ± 5.19	2.43 ± 1.39	0.14 ± 0.05	0.10 ± 0.23	0.24 ± 0.29
20:5(n-3)	10.44 ± 2.00	12.87 ± 12.13	11.54 ± 1.76	10.66 ± 1.69	6.97 ± 3.45	11.18 ± 5.66	11.86 ± 6.52	5.14 ± 2.77	6.00 ± 5.02	7.81 ± 3.71
22:6(n-3)	2.85 ± 2.42	8.98 ± 5.79	11.82 ± 3.64	5.18 ± 2.76	9.61 ± 5.77	3.60 ± 1.85	2.67 ± 1.50	10.95 ± 10.92	6.10 ± 6.26	11.11 ± 6.50
Branched	1.52 ± 0.66	1.10 ± 0.76	2.01 ± 0.38	1.53 ± 0.63	0.72 ± 0.59	6.78 ± 3.10	2.76 ± 1.44	0.79 ± 0.07	1.44 ± 0.64	0.34 ± 0.24

Table 5
Mean ± SD relative abundance (mol% of total fatty alcohols) of key fatty alcohol groups identified in benthic invertebrate and copepod samples. Fatty alcohol groups with median relative abundances of <1 % in either benthic or copepod samples have been excluded. Poly. = Polychaeta; Amph. = Amphipoda; Deca. = Decapoda; Isop. = Isopoda; Mysi. = Mysidacea; Holo. = Holothuroidea; Ophi. = Ophiuroidea; Chae. = Chaetognatha; *C. fin.* = *Calanus finmarchicus*; *C. hyp.* = *Calanus hyperboreus*. Header text below taxa shows sample depth range (m).

	Poly. 1254–5414	Amph. 1254–5414	Deca. 2328–2587	Isop. 1254–2551	Mysi. 2328–2551	Holo. 2328–5414	Ophi. 1254–1255	Chae. 1254–2587	*C. fin.* 0–1255	*C. hyp.* 0–2587
n	3	18	5	3	7	12	5	3	12	19
14:0	3.77 ± 3.09	5.37 ± 8.97	2.58 ± 3.77	0.17 ± 0.29	0.43 ± 0.37	7.43 ± 9.32	4.93 ± 4.05	3.59 ± 3.44	2.86 ± 1.72	8.44 ± 7.41
16:0	30.50 ± 31.92	13.45 ± 12.65	5.21 ± 3.81	18.74 ± 17.13	4.32 ± 4.35	11.31 ± 7.64	6.23 ± 4.94	19.38 ± 7.17	6.74 ± 2.62	9.86 ± 6.19
16:1	0.00 ± 0.00	1.01 ± 1.74	1.40 ± 1.36	0.00 ± 0.00	0.23 ± 0.31	0.36 ± 1.26	2.95 ± 3.83	3.01 ± 3.13	3.60 ± 2.79	2.17 ± 2.00
18:1	0.00 ± 0.00	5.23 ± 7.77	5.44 ± 5.93	0.00 ± 0.00	4.94 ± 9.35	4.39 ± 7.45	19.38 ± 27.16	4.02 ± 5.27	4.27 ± 2.65	1.67 ± 1.02
20:1	6.40 ± 11.08	12.18 ± 11.11	14.35 ± 8.66	6.10 ± 10.56	18.03 ± 13.63	4.68 ± 5.92	10.82 ± 4.42	26.29 ± 12.49	34.27 ± 5.59	29.24 ± 5.71
22:1	18.14 ± 31.42	35.91 ± 25.83	36.34 ± 24.60	22.80 ± 39.48	51.05 ± 28.01	8.67 ± 16.94	31.99 ± 34.07	33.61 ± 3.72	44.90 ± 9.26	45.99 ± 9.98
24:1	0.00 ± 0.00	4.68 ± 6.03	2.31 ± 2.44	0.70 ± 1.21	1.58 ± 3.08	0.05 ± 0.19	0.70 ± 1.00	2.24 ± 2.09	1.68 ± 4.02	0.71 ± 0.32

3.4. Lipid composition and biomarker changes with depth

The relative abundances of *Calanus* spp. lipid biomarkers, PUFA, and total lipid concentrations in *Calanus* spp. or the benthos were not influenced by depth (Fig. 8; linear regression, $p > 0.05$ in all cases).

3.5. Stable isotope analyses

Bulk $\delta^{15}N$ signatures varied significantly among benthic taxa (ANOVA: $F_{6,75} = 22.27$, $p < 0.001$; Fig. 9). Post hoc comparisons indicated that the holothurians (7.21 ± 1.37 ‰) were isotopically lighter compared to all other benthic taxa except for ophiuroids (8.88 ± 0.57 ‰) ($p < 0.05$). Amphipods (11.72 ± 1.82 ‰), decapods (11.95 ± 1.09 ‰) and mysids (11.45 ± 1.36 ‰) also displayed heavier signatures compared to ophiuroids ($p < 0.05$). Bulk $\delta^{15}N$ signatures were highly variable in amphipod samples, ranging from 7.79 to 15.23 ‰. This variability was largely driven by species-specific differences (Table 6). Except for holothurians, the mean $\delta^{15}N$ signatures of all benthic taxa were heavier than the reference $\delta^{15}N$ signatures for *C. finmarchicus* and *C. hyperboreus* (Fig. 9). The trophic level of benthic taxa ranged from 1.73 ± 0.36 in holothurians to 2.92 ± 0.48 in amphipods. Most benthic taxa exhibited trophic levels between 2 and 3 (Fig. 9).

4. Discussion

The *Calanus* spp. seasonal lipid pump (SLP) has recently generated substantial interest in the context of deep-sea carbon sequestration. By contrast, its allied contribution to the trophic ecology of bathyal and abyssal benthic communities has received far less attention. The analyses presented herein demonstrate a clear connection between pelagic *Calanus* spp. and deep-sea benthic ecosystems within the Arctic Fram Strait.

4.1. Lipid profiles and general trophic ecology

The lipid profiles of *Calanus finmarchicus* and *Calanus hyperboreus* featured similar levels of monounsaturated fatty acids and fatty alcohols (Table 3), both pools of which contained large amounts of C20:1 and C22:1. These findings are consistent with previous observations (see Table 2 in Lee et al., 2006). Large amounts of fatty alcohols denote the presence of wax ester lipid stores, which are comprised of fatty acids esterified to fatty alcohols. Wax esters are highly stable energy stores and feature unique biophysical properties that are thought to aid in buoyancy regulation, making them well-suited for supporting *Calanus* spp. during their diapause (Lee et al., 2006; Pond, 2012). However, fatty alcohols need to be oxidised into fatty acids before they can be used to generate ATP (Sargent and Falk-Petersen, 1988), and many other invertebrates therefore use alternative energy storage lipids (e.g., triacylglycerols) that consist of only fatty acids (Lee et al., 2006). Indeed, the lipid profiles of analysed benthic taxa were dominated by monounsaturated fatty acids and featured only low levels of fatty alcohols (Table 3), potentially reflecting the different storage lipids used by benthic invertebrates and *Calanus* spp. (Bühring and Christiansen, 2001; Lee et al., 2006; Drazen et al., 2008).

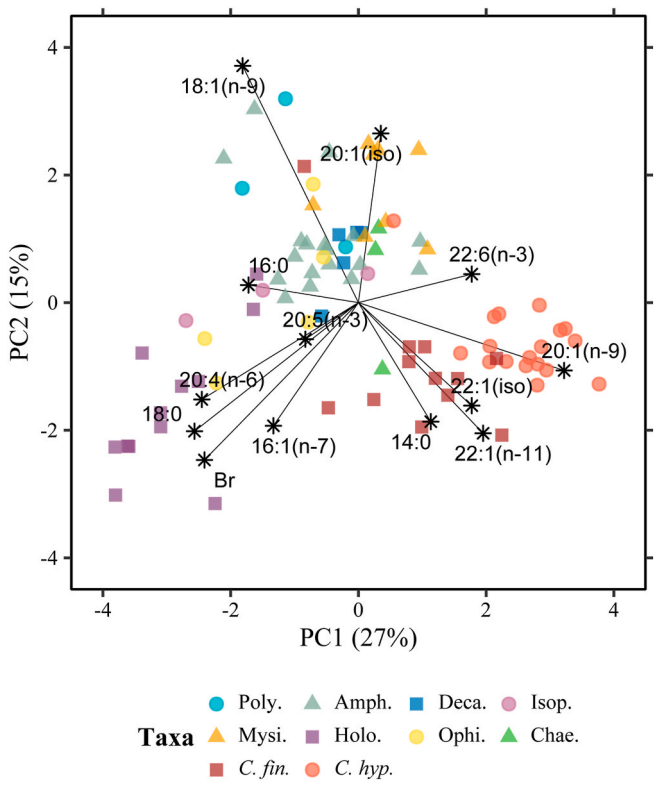

Fig. 5. Principal component analysis plot showing variation in the relative abundance (mol%) of different fatty acids and how fatty acid compositions differed among taxa (taxa and water depth collectively explained 47.63 % of this variability, taxa accounted for 46.01 %). Points represent individual samples. Poly. = Polychaeta; Amph. = Amphipoda; Deca. = Decapoda; Isop. = Isopoda; Mysi. = Mysidacea; Holo. = Holothuroidea; Ophi. = Ophiuroidea; Chae. = Chaetognatha; *C. fin.* = *Calanus finmarchicus*; *C. hyp.* = *Calanus hyperboreus*.

The monounsaturated fatty acid 18:1(n-9) was particularly prevalent in all benthic taxa, suggesting that these animals are opportunistic omnivores/carnivores that could be feeding on organic matter through a range of filter-feeding, predatory, or scavenging strategies (Lehtiniemi et al., 2002; Dalsgaard et al., 2003; Kelly and Scheibling, 2012; Connelly et al., 2014; Parzanini et al., 2018; Käß et al., 2019; Schmittmann et al., 2024). Despite still containing high levels of 18:1(n-9), holothurians featured distinct lipid profiles with relatively high levels of sterols, branched fatty acids, and 20:4(n-6) (Tables 3 and 4). This likely reflects their ingestion of sediment-dwelling microorganisms and detritus (Howell et al., 2003; Suhr et al., 2003; Hudson et al., 2004; Neto et al., 2006; Kelly and Scheibling, 2012) and their use of sterols to mitigate autotoxicity from the saponins they produce to deter predators (Claereboudt et al., 2018). Furthermore, trophic level estimations from the $\delta^{15}N$ signatures provided evidence to suggest that holothurians predominantly fed on primary producers/detritus, whereas all other benthic taxa relayed more heavily on omnivory/carnivory. It should be noted that elevated 18:1(n-9) levels and $\delta^{15}N$ values may arise from prolonged periods of starvation (Gontikaki et al., 2011; Mayor et al., 2013), which can complicate trophic interpretations. Nonetheless, the idea that the analysed taxa formed three broad groupings based on their physiology and trophic strategies (*Calanus* spp.; holothurians; other benthos), was also supported by principal component analysis of the lipid homologous group data (Fig. 4) and the fatty acid data (Fig. 5), both of which illustrated three clusters around these taxonomic groupings.

4.2. Evidence for Calanus-benthos trophic interactions

Calanus spp. lipid biomarkers were present at moderate to high levels within all selected benthic taxa (means = 11.18–29.27 mol%), strongly suggesting that *Calanus* spp.-derived organic matter represents an important dietary component for deep-sea benthos within the Fram Strait. Previous studies have drawn similar conclusions after reporting high levels of C20:1 and C22:1 moieties in benthic mysids, ophiuroids, amphipods, and decapod shrimps found at shelf to bathyal depths within Arctic regions (Graeve et al., 1997; Richoux et al., 2005; Søreide et al., 2013; Connelly et al., 2014; McGovern et al., 2018; Parzanini et al., 2018). High levels of *Calanus* spp. lipid biomarkers have also been reported in the tissues of the predatory pelagic copepod, *Paraeuchaeta* spp., sampled from bathyal depths within the Fram Strait (Laakmann et al., 2009), further highlighting the contribution of *Calanus* spp. to the ecology of cold-water deep-sea ecosystems. Nevertheless, by highlighting the ubiquity of C20:1 and C22:1 moieties across all selected taxa and bathyal–abyssal sample depths, our results underscore the apparently widespread nature of the trophic connection between pelagic *Calanus* spp. and deep-sea benthic animals.

Among the benthic taxa analysed, mysid (*Boreomyis* spp.) and chaetognath (*Heterokrohnia* sp.) specimens exhibited the highest levels of C20:1 and C22:1 fatty acids and alcohols (Tables 4 and 5). Chaetognaths are known to predate directly on copepods (Connelly et al., 2014), whereas mysids are generally considered to be omnivorous planktivores that can switch between filter feeding and active raptorial predation, the latter becoming more common in larger individuals (Viherluoto and Viitasalo, 2001; Lehtiniemi et al., 2002; Oliveira et al., 2023). Substantial consumption of *Calanus* spp.-derived organic matter

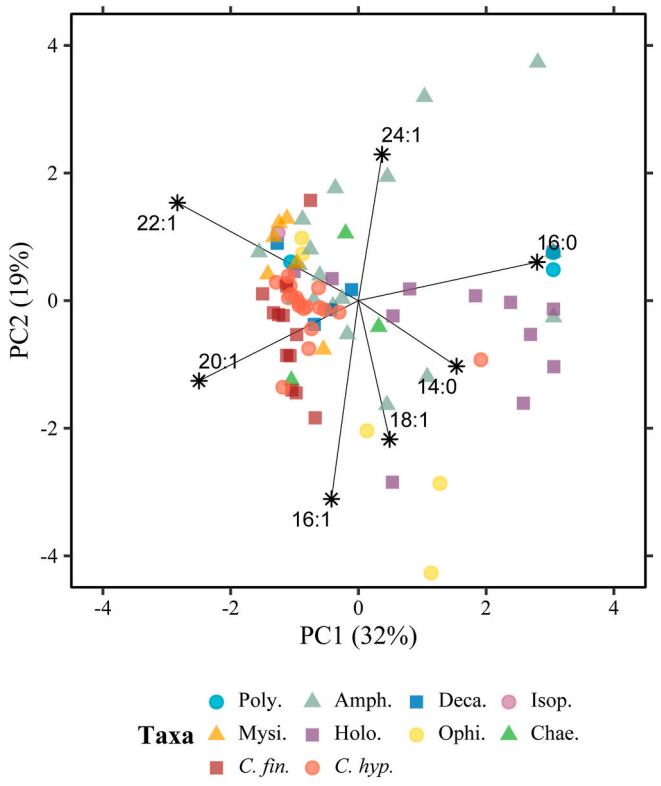

Fig. 6. Principal component analysis plot showing variation in the relative abundance (mol%) of different fatty alcohols and how fatty alcohol compositions differed among taxa (taxa explained 25.25 % of the variability). Points represent individual samples. Poly. = Polychaeta; Amph. = Amphipoda; Deca. = Decapoda; Isop. = Isopoda; Mysi. = Mysidacea; Holo. = Holothuroidea; Ophi. = Ophiuroidea; Chae. = Chaetognatha; *C. fin.* = *Calanus finmarchicus*; *C. hyp.* = *Calanus hyperboreus*.

by mysids aligns well with previous studies. For example, copepods are key prey for the bathyal mysid *Boreomysis arctica* in the western Mediterranean (Cartes and Sorbe, 1998; Cartes, 2011), and high levels of *Calanus* spp. lipid biomarkers (up to 33.1 mol%) were reported in Arctic mysids collected from 240 m in Conception Bay, Newfoundland (Richoux et al., 2005) and between 20 and 500 m on the Beaufort Sea Shelf (Connelly et al., 2014). The mysids examined herein lacked obvious raptorial appendages (Fig. 3) and may have assimilated *Calanus* spp. lipid biomarkers through the consumption of carcasses and/or faecal pellets.

Although the mean relative abundance of *Calanus* spp. biomarkers was comparably low in amphipod specimens, the high densities of amphipods observed at HAUSGARTEN stations (Soltwedel et al., 2009) suggests that this taxon could still consume substantial quantities of *Calanus* spp.-derived material at a population level. Biomarker and stable isotope data within this taxon were also highly variable, which likely reflects the diverse and opportunistic feeding ecology of these animals (Sainte-Marie and Brunel, 1985; Legeżyńska, 2008; Connelly et al., 2014). The highest relative abundances of *Calanus* spp. biomarkers were observed in high trophic level (>12.5 δ^{15}N) amphipod taxa known to scavenge on nekton, including Stegocephalidae (family) sp., *Eurythenes* sp., and *Anonyx nugax* (Legeżyńska et al., 2012; Schmittmann et al., 2024). *Halirages* spp. featured notably lower levels (<10 mol%) of *Calanus* spp. biomarkers and lower δ^{15}N values. Deep-sea members of this genus are often suspension feeders and certain species (including *H. spongiae*) associate with sponges to enhance particle capture success (Legeżyńska et al., 2012; Lörz et al., 2024). Foraging behaviours that result in detecting *Calanus* prey/carcasses are thus probably more limited in *Halirages* spp. compared to more carnivorous species. Specimens of *Rhachotropis* sp. represented a mid-point, featuring moderate *Calanus* biomarkers (~18 mol%) and δ^{15}N values roughly equal to the third tropic level. Interestingly, previous gut content and lipid analyses have already uncovered *Rhachotropis* spp. as predators that feed on live calanoid and harpacticoid copepods (Sainte-Marie and Brunel, 1985; Connelly et al., 2014). Taken together, these results indicate that amphipod species foraging for carcasses might be more likely to encounter *Calanus* spp.-derived lipids compared to those feeding on suspended organic matter or seeking live prey. Future work could look at species-specific patterns in more detail, with more replicates per species, to confirm this conclusion.

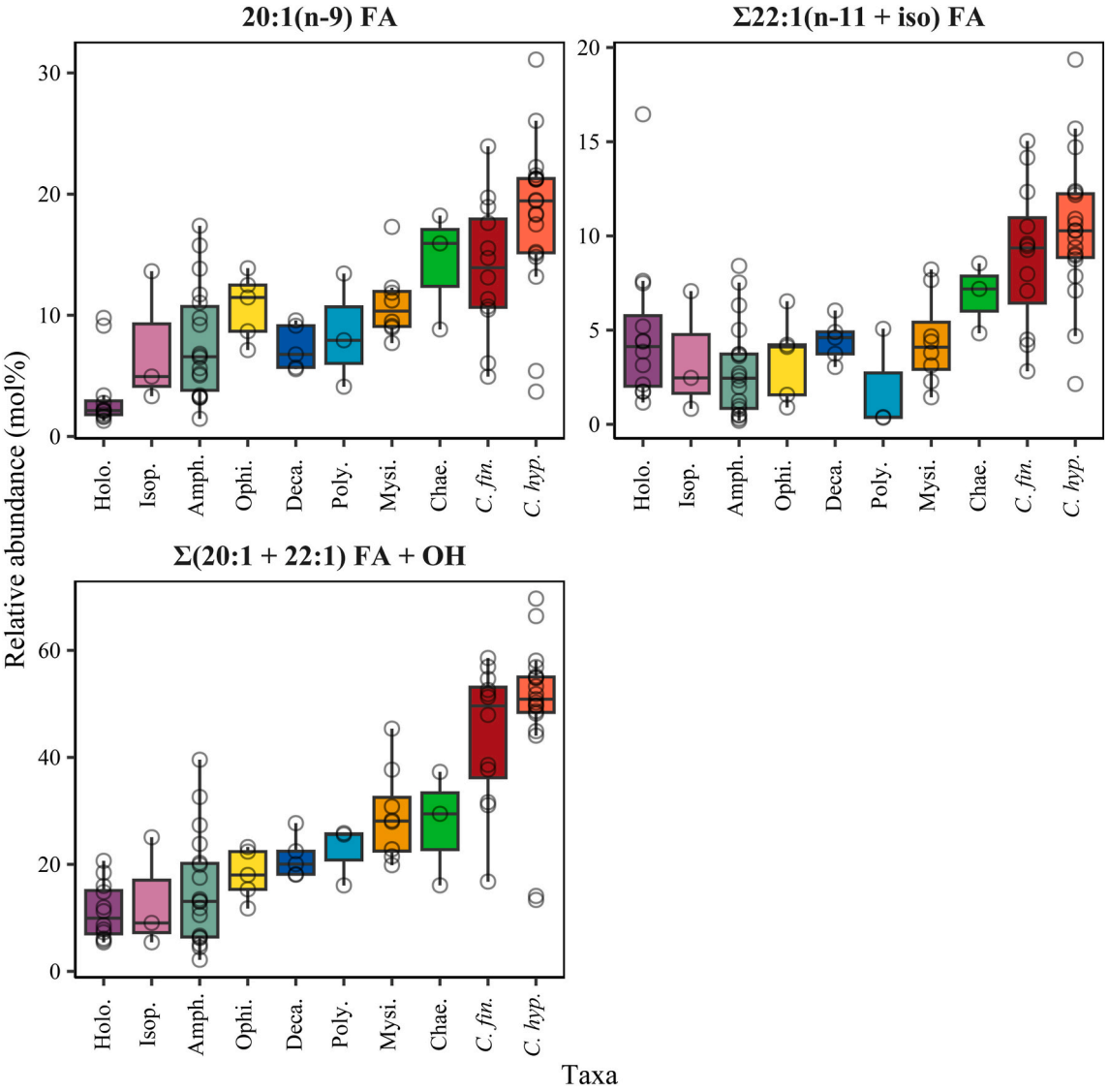

Fig. 7. The relative abundances of key *Calanus* spp. biomarkers among different taxa. Relative abundances of the fatty acid 20:1(n-9) and the sum of the fatty acids 22:1(n-11) + 22:1(iso) were converted to mol% of total fatty acids within each sample. Relative abundances of total 20:1 and 22:1 moieties were converted to mol% of total fatty acids and alcohols within each sample. Poly. = Polychaeta; Amph. = Amphipoda; Deca. = Decapoda; Isop. = Isopoda; Mysi. = Mysidacea; Holo. = Holothuroidea; Ophi. = Ophiuroidea; Chae. = Chaetognatha; *C. fin.* = *Calanus finmarchicus*; *C. hyp.* = *Calanus hyperboreus*.

Table 6
Lipid content, *Calanus* spp. biomarker levels, and bulk $\delta^{15}N$ signatures of benthic invertebrate and copepod samples resolved to a family–species level. Data are reported as means ± SD (unless replicates are absent). Calanus spp., which were already resolved to a species level in all prior analyses, are instead resolved into three depth ranges. TL = total lipid dry weight per individual; TLC = total lipid concentration (dry weight); Holo. = Holothuroidea; Isop. = Isopoda; Amph. = Amphipoda; Ophi. = Ophiuroidea; Deca. = Decapoda; Poly. = Polychaeta; Mysi. = Mysidacea; Chae. = Chaetognatha; *C. fin.* = *Calanus finmarchicus*; *C. hyp.* = *Calanus hyperboreus*; n = number of samples used for lipid or stable isotope analyses. Sample depth range is shown below the species name.

Taxa	Species/Depth (m)	n	TL (μg ind^{-1})	TLC (mg g^{-1})	C20:1 + C22:1 (mol%)	C20:1 + C22:1 (mg g^{-1})	C20:1 + C22:1 (μg ind^{-1})	$\delta^{15}N$
Holo.	*Elpidia* sp. 2328–5414	19	32.09 ± 49.28	2.22 ± 1.54	11.18 ± 5.22	0.17 ± 0.15	2.23 ± 2.82	7.22 ± 1.37
Isop.	*Eurycope* sp. 1254–2551	3	73.98 ± 57.76	61.87 ± 47.96	13.18 ± 10.45	6.25 ± 3.27	14.04 ± 17.30	10.29 ± 1.21
Amph.	Ampipoda (order) sp. 1254–1255	1	-	-	-	-	-	7.79
	Anonyx nugax 5409–5414	1	4914.74	386.99	20.28	85.14	1081.22	14.74
	Eurythenes sp. 2328–2336	2	3338.44	76.05	23.81	18.95	831.74	14.05 ± 0.77
	Halirages cf. *cainae* 1254–1255	1	1455.65	50.02	6.37	3.36	97.81	9.75
	Halirages sp. 2545–5414	6	1222.04 ± 609.61	50.69 ± 41.66	16.45 ± 11.45	12.20 ± 14.44	211.50 ± 225.53	11.15 ± 1.22
	Halirages spongiae 2328–2383	5	3130.58 ± 2570.94	38.54 ± 25.52	9.15 ± 4.13	4.26 ± 4.37	352.31 ± 434.49	10.19 ± 0.30
	Rachotropis sp. 1254–2587	7	2009.44 ± 1644.45	95.85 ± 40.55	17.83 ± 8.96	20.76 ± 18.39	462.54 ± 496.93	11.70 ± 0.80
	Stegocephalidae (family) sp. 2328–2336	2	909.82	104.58	39.55	42.83	372.63	12.85 ± 0.76
	Cyphocaris cf. *bouvieri* 2328–2336	3	158.36 ± 205.85	39.93 ± 50.98	4.40 ± 3.17	1.02 ± 1.11	4.00 ± 4.56	14.13 ± 1.42
	All above	28	2065.06 ± 1828.52	82.39 ± 85.47	15.22 ± 10.39	17.21 ± 22.53	374.88 ± 408.43	11.72 ± 1.82
Ophi.	*Ophiocten* sp. 1254–1255	7	227.79 ± 187.27	19.73 ± 15.57	18.15 ± 4.81	3.95 ± 3.93	44.98 ± 40.98	8.88 ± 0.57
Deca.	*Bythocaris* sp. 2328–2587	7	4245.71 ± 4004.52	49.34 ± 34.63	21.28 ± 4.01	10.20 ± 6.70	880.46 ± 787.40	11.95 ± 1.09
Poly.	*Aglaophamus* cf. *malmgreni* 1254–1255	1	22.29	37.14	25.57	9.19	5.51	10.21
	Ophelina sp. 2560–5414	4	10.69 ± 5.78	40.80 ± 35.70	20.95 ± 6.92	8.21 ± 8.20	2.99 ± 2.25	11.68 ± 1.31
	All above	5	14.56 ± 7.84	39.58 ± 25.33	22.49 ± 5.57	8.54 ± 5.83	3.07 ± 2.16	11.38 ± 1.31
Mysi.	*Boreomysis* sp. (white) 2328–2551	6	5543.05 ± 1440.97	130.28 ± 47.77	29.82 ± 6.20	42.45 ± 22.67	1709.34 ± 439.39	12.67 ± 0.67
	Boreomysis sp. (red) 2328–2551	7	4507.89 ± 4552.66	95.25 ± 76.73	28.72 ± 11.67	33.62 ± 32.87	1567.79 ± 1613.54	10.41 ± 0.75
	All above	13	5025.47 ± 3174.73	112.77 ± 62.06	29.27 ± 8.67	38.03 ± 26.56	1638.57 ± 1097.39	11.45 ± 1.36
Chae.	*Heterokrohnia* sp. 1254–2587	3	72.04 ± 31.53	61.16 ± 49.03	27.60 ± 10.72	19.89 ± 16.74	23.03 ± 14.24	-
C. fin.	<200	11	13.92 ± 10.74	101.36 ± 62.42	44.71 ± 13.35	46.91 ± 24.43	6.81 ± 5.57	-
	200–1000	0	-	-	-	-	-	-
	>1000	1	4.89	16.52	37.73	6.33	1.87	-
C. hyp.	<200	10	363.28 ± 260.73	152.09 ± 74.30	46.29 ± 18.52	71.68 ± 43.83	193.17 ± 156.81	-
	200–1000	6	222.00 ± 167.39	161.02 ± 116.08	53.49 ± 7.22	87.15 ± 55.38	119.88 ± 77.40	-
	>1000	4	359.94 ± 402.19	157.59 ± 10.71	50.28 ± 0.58	85.99 ± 5.02	193.17 ± 156.81	-

Ophiuroid specimens (*Ophiocten* sp.) exhibited notably high levels of the fatty acid 20:1(n-9), yet their $\delta^{15}N$ signatures indicated that they were only opportunistic carnivores and may have also consumed substantial amounts of phytodetrital material (Pearson and Gage, 1984; Howell et al., 2003). Ophiuroids were exclusively collected at the shallowest benthic station (1255 m) and could have therefore fed more intensely on *Calanus* spp.-derived organic matter given their increased proximity to the depth at which *Calanus* spp. typically overwinter (Heath et al., 2008; Baumgartner and Tarrant, 2017), and to surface waters where non-diapausing populations produce faecal pellets. This is further supported by previous studies on Arctic food webs reporting high levels of *Calanus* spp. biomarkers in deep-sea echinoderms, including ophiuroids, suggesting that certain groups employ suspension-feeding or opportunistic scavenging on copepods (Graeve et al., 1997; Howell et al., 2003; Søreide et al., 2013; Parzanini et al., 2018). As such, the comparably low trophic level of ophiuroid specimens might suggest that when carnivory is employed, low trophic level prey (including *Calanus* spp.) are targeted (Iken et al., 2005; Søreide et al., 2008).

Benthic taxa showed differing trends in the relative abundances of the *Calanus* spp. biomarkers 20:1(n-9) and C22:1 within their fatty acid pools (Fig. 7). For instance, ophiuroids and polychaetes displayed relatively high levels of 20:1(n-9) but reduced levels of C22:1 fatty acids compared to other taxa, whereas decapods and holothurians exhibited increased levels of C22:1. This pattern may reflect taxa-specific differences in how efficiently benthic animals assimilate ingested wax esters and metabolise their own lipid stores. Notably, the fatty alcohol pool of *Calanus* spp. lipids was dominated by C22:1 compounds (Table 4), while C20:1(n-9) was more abundant in the fatty acid pool (Table 5). Benthic taxa that ingest *Calanus* spp. and efficiently oxidise their fatty alcohols to fatty acids may therefore assimilate greater levels of C22:1 into their tissues, compared to those that poorly oxidise fatty alcohols. Alternatively, different taxa may catabolise certain fatty acids at different rates (e.g., Mayor et al., 2011, 2022), giving rise to variable ratios of 20:1(n-9) and C22:1 fatty acids within their tissues. Different trophic pathways could also influence the relative abundances of *Calanus* spp. biomarkers ingested by each taxon, though no clear link between feeding ecology and the dominance of 20:1(n-9) or C22:1 fatty acids was apparent in this study.

The clear evidence for trophic connectivity between *Calanus* spp. and multiple deep-sea benthic taxa raises questions about the quantitative importance of this linkage for the ecology of the receiving ecosystem.

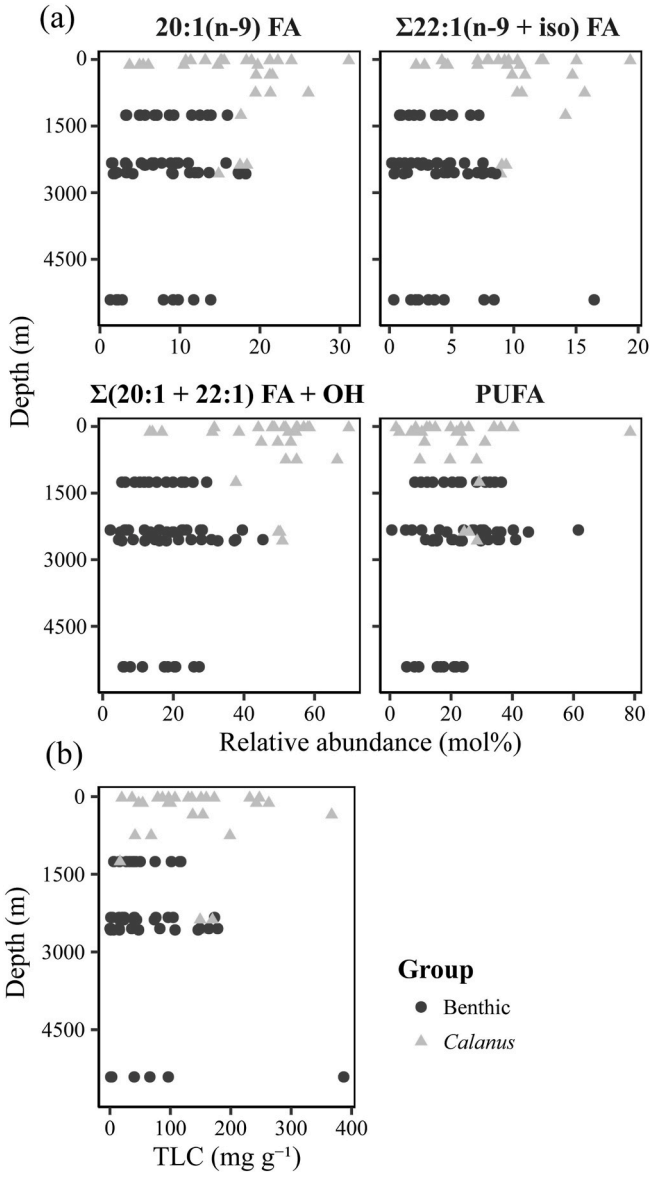

Fig. 8. The relative abundances of lipid variables in benthic taxa (1255–5409 m) and *Calanus* spp. (0–2560 m) versus depth. (a) Relative abundances of *Calanus* spp. biomarkers (fatty acid 20:1(n-9), sum of the fatty acids 22:1(n-11) + 22:1(iso), and sum of 20:1 and 22:1 fatty acids and alcohols) and polyunsaturated fatty acids (PUFA). (b) Total lipid concentrations (TLC: dry weight). No significant relationship between any lipid variable and water depth were apparent (benthos and *Calanus* spp. groups treated independently; ANOVA, $p > 0.05$ in all cases).

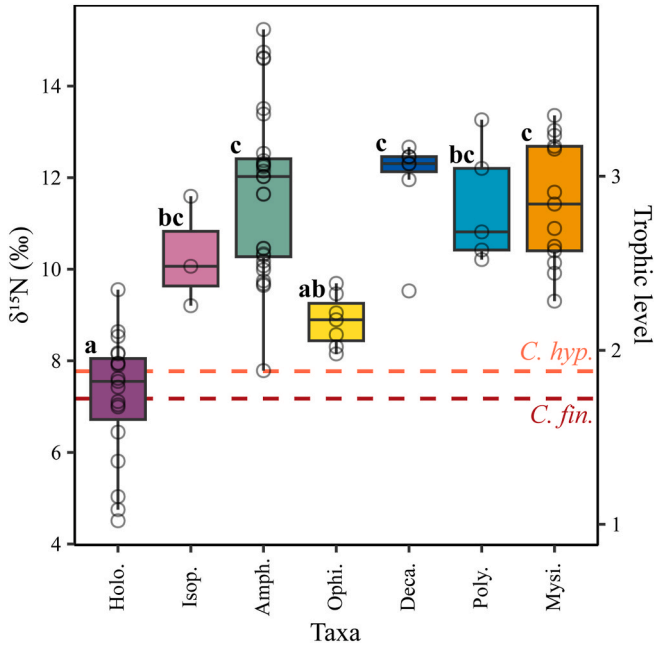

Fig. 9. Comparison of the bulk $\delta^{15}N$ signatures and trophic levels among different benthic taxa. Trophic levels were estimated using a $\delta^{15}N_{baseline}$ value of 4.43 ‰ and a $\delta^{15}N_{enrichment}$ factor of 3.80 ‰ per trophic level (Bergmann et al. 2009 and references therein). Horizontal lines reference the mean $\delta^{15}N$ signatures for *C. finmarchicus* (7.18 ± 0.65 ‰) and *C. hyperboreus* (7.78 ± 0.86 ‰) specimens collected from the Svalbard region in May, as reported by Søreide et al. (2008). ANOVA results demonstrated that bulk $\delta^{15}N$ signatures varied among taxa ($F_{6,75} = 22.27$, $p < 0.001$). Different letters above each boxplot show which groups have significantly different ($p < 0.05$) $\delta^{15}N$ signatures based on Tukey's HSD post hoc analysis (i.e. groups that share a letter were not statistically significantly different). Poly. = Polychaeta; Amph. = Amphipoda; Deca. = Decapoda; Isop. = Isopoda; Mysi. = Mysidacea; Holo. = Holothuroidea; Ophi. = Ophiuroidea; *C. fin.* = *Calanus finmarchicus*; *C. hyp.* = *Calanus hyperboreus*. Note that isotope analyses were not conducted on chaetognath specimens.

However, it remains difficult to quantify the amount of *Calanus* spp.-derived lipid consumed by each benthic taxon because to do so requires detailed understanding of their physiology, particularly with regards to the efficiencies with which they absorb and assimilate C20:1 and C22:1 moieties and the subsequent rates at which these compounds are turned over during routine metabolism. Measuring these physiological parameters should therefore be a key focus of future endeavours to better understand the trophic ecology of deep-sea benthos and their linkages to *Calanus* spp.

4.3. Potential trophic connection routes

The presence of pelagic *Calanus* spp. lipid biomarkers within the tissues of the benthic animals presented herein could have occurred through a range of non-mutually-exclusive routes, which include the consumption of: 1) *Calanus* spp. faecal pellets and exuviae, 2) *Calanus* spp. carcasses following mortality, 3) live *Calanus* spp. in the water column during diapause, 4) carcasses and/or faeces from other animals that feed on *Calanus* spp.

Particulate organic matter is generally considered to be the primary source of food for deep-sea benthic communities (Iken et al., 2005; Parzanini et al., 2018; Käß et al., 2021). This sinking flux can be comprised of various organic sources, including zooplankton faecal pellets (Bathmann et al., 1987; Turner, 2015). Faecal pellets produced by *Calanus* spp. do contain C20:1 and C22:1 fatty acids and fatty alcohols (Harvey et al., 1987; Mayor et al., 2011), and they clearly serve as a vector of organic matter transfer to deep-sea benthic ecosystems in the Fram Strait (Bathmann et al., 1987; Lalande et al., 2016). However, export flux at HAUSGARTEN is relatively low (Bauerfeind et al., 2009), and likely subject to a multitude of mesopelagic detritivores that attenuate this passively sinking organic matter before it reaches bathyal depths (Wexels Riser et al., 2007; Mayor et al., 2014, 2020b). Moreover, copepod faecal pellets typically exhibit lighter $\delta^{15}N$ signatures compared to copepod tissue (Altabet and Small, 1990; Tamelander et al., 2006; Mayor et al., 2011), yet the $\delta^{15}N$ signatures of most benthic specimens analysed in this research were considerably heavier (>3.80 ‰) than typical values for *Calanus* spp. in this region (Søreide et al., 2008, 2013). Combined, these observations suggest that faecal pellets are unlikely to be the main dietary route through which the deep-sea benthos in the Fram Strat encounter *Calanus* spp. biomarkers. We therefore suggest that additional mechanisms of organic matter transfer between *Calanus* spp. and the deep-sea benthos are likely to be in operation.

It is perhaps more likely that benthic animals were feeding on diapausing *Calanus* spp. individuals and/or their carcasses. *Calanus* spp. are thought to predominantly occupy depths <2000 m during diapause (Heath et al., 2008; Falk-Petersen et al., 2009; Baumgartner and Tarrant, 2017), although high abundances of *C. hyperboreus* have previously been documented close to the seafloor at 2300–2500m in the Fram Strait (Auel et al., 2003) and bathymetric distributions >2500 m have been reported for *Calanus* spp. in other Arctic regions (Baumgartner and Tarrant, 2017; Brix et al., 2022). Furthermore, Kvile et al. (2019) demonstrated that the vertical distributions of diapausing *Calanus* spp. deepen with increasing bottom depth, and suggested that *Calanus* spp. may aggregate at the seafloor when the topography limits the maximum depths they can attain. We acknowledge that our benthic specimens were collected during May–June, a period when *Calanus* populations are typically feeding in surface waters and accumulating lipid reserves in preparation to enter diapause from August (Visser et al., 2017; Tarling et al., 2022a). However, we do not know the lipid turnover rates within deep-sea benthic invertebrates, or whether certain moieties are selectively catabolised or retained. It is possible that the high levels of *Calanus* spp. biomarkers detected in benthic taxa are remnants of the previous diapause season. Equally, *Calanus* spp. specimens were collected during our epibenthic sledge deployments at ~1255–2560 m, indicating that a portion of the diapausing population remains in the deep ocean during May and June (Tables 2 and 6).

Identifying whether the benthos relied more heavily on live or dead *Calanus* spp. remains challenging. Previous studies have documented substantial reductions in *Calanus* spp. population sizes between the onset and termination of diapause, with losses primarily attributed to advection or pelagic predators (Bagøien et al., 2001; Gislason et al., 2007; Espinasse et al., 2018). 'Doomed' (Auel et al., 2003) individuals that have failed to exit diapause might also represent an easily captured prey for opportunistic benthic carnivores, particularly if they are still in a dormant state (Ingvarsdóttir et al., 1999; Mayor et al., 2022). Conversely, Daase et al. (2014) reported that 94 % of *Calanus* spp. specimens collected between 300 and 2000 m in the Sofiadjupet basin were dead, possibly due to stress and/or starvation, postulating that *Calanus* spp. carcasses could thus represent a major food source for benthic communities. Potentially supporting the importance of carcasses, the relative abundance of *Calanus* spp. lipid biomarkers did not decline with depth in our study, and moderate levels were still detected in benthic taxa found below 5000 m (namely *Halirages* sp. and *Ophelina* sp.). This lies below the known bathymetric distribution of diapausing *Calanus* spp. (Heath et al., 2008; Baumgartner and Tarrant, 2017) but *Calanus* carcasses could sink from bathyal to abyssal depths prior to complete decomposition, particularly given the slow degradation rates and high sinking velocities of large zooplankton carcasses in cold environments (Daase and Søreide, 2021; Franco-Cisterna et al., 2021; Halfter et al., 2022). The notably high levels of *Calanus* spp. lipid biomarkers detected in scavenging taxa (section 4.2) further indicates that individuals consumed by the benthos were already dead. Nevertheless, inactive *Calanus* spp. that are unable to terminate diapause or reascend to the surface could still be targeted by generalist scavengers, and may sink to water depths below their typical diapause distribution if they fail to regulate their buoyancy (Clark et al., 2012; Pond, 2012; Pond et al., 2012; Schmidt et al., 2025).

In addition to direct consumption, benthic taxa could have encountered *Calanus* spp. biomarkers through indirect trophic interactions by feeding on the carcasses or faeces of other planktivorous taxa. For example, pelagic fish may struggle to digest the high concentrations of wax esters within *Calanus* spp., resulting in the production of faeces containing high concentrations of their lipid biomarkers (Sargent et al., 1977). Furthermore, fish that feed on *Calanus* spp. can also accumulate high levels of C20:1 and C22:1 fatty acids within their tissues (e.g., Maar et al., 2023) which could then be transferred to benthic scavengers that feed on their carcasses. Indeed, recent DNA metabarcoding of the gut contents of deep-sea amphipods at HAUSGARTEN stations within in the Fram Strait indicates that the carcasses of larger pelagic nekton also play an important role in the trophic ecology of this region (Soltwedel et al., 2003; Schmittmann et al., 2024).

Finally, it is important to recognise that C20:1 and C22:1 moieties have been identified in the lipid pools of non-diapausing species of deep-sea calanoid copepods (Bühring and Christiansen, 2001; Kosobokova et al., 2002; Laakmann et al., 2009; Maar et al., 2023). The levels of these biomarkers in deep-sea copepod species are substantially lower than those reported for *Calanus* spp. (Bühring and Christiansen, 2001; Kosobokova et al., 2002; Maar et al., 2023), and their presence in predatory copepods have previously been attributed to the consumption of *Calanus* spp. (Laakmann et al., 2009). As such, it seems likely that *Calanus* spp. are the primary source of these biomarkers in benthic taxa, although additional contributions from other copepod taxa cannot be ruled out.

Based on the evidence presented above and high levels of *Calanus* spp. biomarkers detected in scavenging taxa, we propose that dead or moribund *Calanus* spp. individuals constitute the primary source of *Calanus* spp.-derived lipids in the deep-sea benthos. To test this hypothesis, future research could quantify *Calanus* spp. biomarker concentrations within deep-sea benthic taxa immediately before and after the diapause period, while also performing traditional stomach content analyses and DNA metabarcoding of the stomach contents. Detecting

elevated levels of *Calanus* spp. lipid biomarkers after the diapause period and/or finding intact *Calanus* spp. in the stomach contents would provide support for this interpretation. Furthermore, additional comparisons of *Calanus* spp. biomarker levels between strict necrophages and planktivorous predators may shed light on the importance of live and dead *Calanus* spp. as prey for the deep-sea benthos.

4.4. Implications and uncertainties of Calanus spp.-derived inputs to deep-sea ecosystems

The consumption of *Calanus* spp. by benthic taxa has potential implications for gross long-term carbon sequestration and might partially explain the mismatch between vertical carbon export and benthic demand in the Arctic Ocean (Wiedmann et al., 2020). Within the Fram Strait, the seasonal migration of *C. finmarchicus* and *C. hyperboreous* is estimated to transport 2.35 and 3.62 gC m^{-2} y^{-1} into the deep-sea, respectively (Visser et al., 2017; Tarling et al., 2022a). This flux is calculated as the sum of CO_2 released from *Calanus* spp. as they respire during diapause and the carbon contained in tissue that remains in the deep-sea following mortality (Visser et al., 2017; Tarling et al., 2022a). Population mortality rates are an acknowledged uncertainty in these estimates and only contribute towards ~15 % of the total SLP carbon flux (Visser et al., 2017; Tarling et al., 2022a). Quantifying the rates and causes of *Calanus* spp. mortality during diapause has been the focus of numerous studies (e.g., Bagøien et al., 2001; Gislason et al., 2007; Espinasse et al., 2018; Pinti et al., 2023), yet the potential consumption of *Calanus* spp. by benthic predators is seldom considered.

If benthic taxa predate on live diapausing individuals, then this trophic interaction could directly influence *Calanus* spp. mortality rates and thus the proportion of carbon that remains at depth after the diapause season has ended. Conversely, the interaction is unlikely to have major implications for carbon flux estimates if benthic taxa primarily consume *Calanus* spp. carcasses; the carbon content of *Calanus* spp. individuals that die during diapause is considered sequestered regardless of whether their carcasses are consumed or not. Such consumption may, however, still influence the residence time of *Calanus* spp.-derived carbon within the deep ocean. For example, deep-sea benthos are typically restricted to their respective depth zones, meaning that carbon transferred to benthic consumers might exhibit a longer residence time compared to carbon routed through pelagic predators or remineralised in the water column (Pinti et al., 2023). On the other hand, supra-benthic consumers may reduce the gross sequestration of carbon by intercepting *Calanus* spp. carcasses before they reach the sediment. Deep-sea amphipods can exhibit particularly broad bathymetric distributions and might even return *Calanus* spp.-derived carbon to shallower depths (Sainte-Marie, 1992; Lacey et al., 2018). Clarifying the route(s) through which *Calanus* spp.-derived organic matter enters the deep-sea benthic ecosystem, together with quantifying the rates at which this material is consumed and turned over (as noted in section 4.2), are key to constraining its role in carbon sequestration.

Beyond transporting carbon, a potentially more insidious implication of our study is that *Calanus* spp. may also be acting as a vector for the transport of lipid-soluble heavy metals and persistent organic pollutants (POPs) into deep-sea benthic ecosystems. Contaminants such as dichloro-diphenyl-trichloroethane (DDT), polychlorinated biphenyls (PCBs), and chlordane are routinely found in surface populations of *Calanus* spp. and other lipid-rich Arctic zooplankton (Ritterhoff and Zauke, 1997; Hargrave et al., 2000; Fisk et al., 2001; Hallanger et al., 2011). If *Calanus* spp. accumulate these surface-derived contaminants in their lipids prior to diapause, benthic animals that consume their tissues may also be exposed to elevated concentrations. However, we are unaware of any study that has examined whether high levels of anthropogenic contaminants are found in diapausing *Calanus* spp. This potential 'pollutant-pump' pathway may be of increasing concern following the ongoing poleward expansion of human infrastructure and activities (e.g., tourism, shipping, oil and gas exploration, etc.) in the Arctic Ocean (Pouch and Zaborska, 2015; Hansen et al., 2024).

4.5. Conclusion

Our findings highlight the existence of a trophic coupling between seasonally migrating *Calanus* spp. and deep-sea benthic ecosystems within the Arctic Fram Strait. Whilst the specific pathways for this coupling and its quantitative importance for carbon sequestration currently remain uncertain, the evidence presented in this study indicates that *Calanus* spp. play an important role in supporting the ecological functioning of high-latitude deep-sea benthic ecosystems.

CRediT authorship contribution statement

Dewi Ford: Writing – original draft, Visualization, Methodology, Investigation, Formal analysis. **Katrin Linse:** Writing – original draft, Visualization, Project administration, Methodology, Investigation, Funding acquisition, Formal analysis, Data curation, Conceptualization. **Sabena Jane Blackbird:** Writing – review & editing, Methodology, Investigation. **Anna K. Wadsworth:** Writing – review & editing, Visualization, Formal analysis. **Jennifer J. Freer:** Writing – review & editing, Investigation. **Rachel Jeffreys:** Writing – review & editing, Methodology, Investigation. **Lydia Anastasia Schmidt:** Writing – review & editing, Visualization, Investigation. **Daniel J. Mayor:** Writing – original draft, Visualization, Supervision, Resources, Project administration, Methodology, Investigation, Funding acquisition, Formal analysis, Data curation, Conceptualization.

Declaration of competing interest

The authors declare that they have no known competing financial interests or personal relationships that could have appeared to influence the work reported in this paper.

Acknowledgements

We thank captain Thomas Wunderlich and his crew for their support during PS136. KL and LAS are grateful to PSO Thomas Soltwedel for his invite to participate in the expedition as part of the AWI Deep Sea group and for the ship time to deploy the EBS. We sincerely thank Emilie Breunig for EBS and CTD support, and Alexandra Aves and Maximilian Schrade for help with the live EBS sample sorting. JJF is grateful to Kim Vane and Barbara Niehoff for their help in copepod sampling and identification whilst on board, and to Sinhue Torres-Valdes who assisted JJF's participation in the expedition via the BIOPOLE programme. We are also grateful to those involved with the ALONGate project for their cooperation with BIOPOLE and to the DZMB (Senckenberg) team for their sample management. Saskia Brix (who was support via the Leibniz foundation and the ALONGate project) played a vital role towards this research by providing access to the sampling opportunity. This study was supported by grant no. AWI_PS136_01. The contributions of KL, JJF and DJM were supported by the BIOPOLE National Capability Multicentre Round 2 funding from the Natural Environment Research Council (grant no. NE/W004933/1). DJM also received funding from the European Union under grant agreement no. 101083922 (OceanICU) and UK Research and Innovation (UKRI) under the UK government's Horizon Europe funding guarantee [grant number 10054454, 10063673, 10064020, 10059241, 10079684, 10059012, 10048179]. Views and opinions expressed are however those of the author(s) only and do not necessarily reflect those of the European Union or European Research Executive Agency. Neither the European Union nor the granting authority can be held responsible for them. This paper contributes to the BIOPOLE, OceanICU, IceAGE, ALONGate and HAUSGARTEN programmes. Finally, we thank the reviewers for their time and valuable feedback.

Appendix A. Supplementary data

Supplementary data to this article can be found online at https://doi.org/10.1016/j.dsr2.2026.105644.

Data availability

The expedition metadata from the AWI lead expedition PS136 are deposited in PANGAEA and DOIs referenced in the publication. The data from the lipid and stable isotope analyses of this study are deposited at the UK Polar Data Centre (https://doi.org/10.5285/E115D087-E3E4-4794-B4E0-18262B8E6400).

References

Altabet, M.A., Small, L.F., 1990. Nitrogen isotopic ratios in fecal pellets produced by marine zooplankton. Geochem. Cosmochim. Acta 54 (1), 155–163.

Anderson, T.R., Hessen, D.O., Gentleman, W.C., Yool, A., Mayor, D.J., 2022. Quantifying the roles of food intake and stored lipid for growth and development throughout the life cycle of a high-latitude copepod, and consequences for ocean carbon sequestration. Front. Mar. Sci. 9, 928209.

Anderson, T.R., Hessen, D.O., Gentleman, W.C., Yool, A., Mayor, D.J., 2024. Optimal phenology of life history events in *Calanus finmarchicus*: exit from diapause in relation to interannual variation in spring bloom timing and predation. J. Plankton Res. 46 (4), 439–451.

Auel, H., Klages, M., Werner, I., 2003. Respiration and lipid content of the Arctic copepod *Calanus hyperboreus* overwintering 1 m above the seafloor at 2,300 m water depth in the Fram Strait. Mar. Biol. 143, 275–282.

Bagøien, E., Kaartvedt, S., Aksnes, D.L., Eiane, K., 2001. Vertical distribution and mortality of overwintering *Calanus*. Limnol. Oceanogr. 46 (6), 1494–1510.

Bathmann, U., Noji, T., Voss, M., Peinert, R., 1987. Copepod fecal pellets: abundance, sedimentation and content at a permanent station in the Norwegian Sea in May/June 1986. Mar. Ecol. Prog. Ser. 45–51.

Bauerfeind, E., Nöthig, E.-M., Beszczynska, A., Fahl, K., Kaleschke, L., Kreker, K., Klages, M., Soltwedel, T., Lorenzen, C., Wegner, J., 2009. Particle sedimentation patterns in the eastern Fram Strait during 2000–2005: results from the Arctic long-term observatory HAUSGARTEN. Deep Sea Res. Oceanogr. Res. Pap. 56 (9), 1471–1487.

Baumgartner, M.F., Tarrant, A.M., 2017. The physiology and ecology of diapause in marine copepods. Ann. Rev. Mar. Sci 9 (1), 387–411.

Bergmann, M., Dannheim, J., Bauerfeind, E., Klages, M., 2009. Trophic relationships along a bathymetric gradient at the deep-sea observatory HAUSGARTEN. Deep Sea Res. Oceanogr. Res. Pap. 56 (3), 408–424.

Boyd, P.W., Claustre, H., Levy, M., Siegel, D.A., Weber, T., 2019. Multi-faceted particle pumps drive carbon sequestration in the ocean. Nature 568 (7752), 327–335.

Brenke, N., 2005. An epibenthic sledge for operations on marine soft bottom and bedrock. Mar. Technol. Soc. J. 39 (2), 10–21.

Brix, S., Kaiser, S., Lörz, A.-N., Le Saout, M., Schumacher, M., Bonk, F., Egilsdottir, H., Olafsdottir, S.H., Tandberg, A.H.S., Taylor, J., 2022. Habitat variability and faunal zonation at the Ægir Ridge, a canyon-like structure in the deep Norwegian Sea. PeerJ 10, e13394.

Bühring, S.I., Christiansen, B., 2001. Lipids in selected abyssal benthopelagic animals: links to the epipelagic zone? Prog. Oceanogr. 50 (1-4), 369–382.

Cartes, J.E., 2011. Temporal changes in lipid biomarkers, especially fatty acids, of the deep-sea crustaceans *Boreomysis arctica* and *Nematoscelis megalops*: implications of their biological cycle and habitat near the seabed. J. Mar. Biol. Assoc. U. K. 91 (4), 783–792.

Cartes, J.E., Sorbe, J., 1998. Aspects of population structure and feeding ecology of the deep-water mysid *Boreomysis arctica*, a dominant species in western Mediterranean slope assemblages. J. Plankton Res. 20 (12), 2273–2290.

Claereboudt, E.J., Eeckhaut, I., Lins, L., Deleu, M., 2018. How different sterols contribute to saponin tolerant plasma membranes in sea cucumbers. Sci. Rep. 8 (1), 10845.

Clark, K., Brierley, A., Pond, D., 2012. Composition of wax esters is linked to diapause behavior of *Calanus finmarchicus* in a sea loch environment. Limnol. Oceanogr. 57 (1), 65–75.

Connelly, T.L., Deibel, D., Parrish, C.C., 2014. Trophic interactions in the benthic boundary layer of the Beaufort Sea shelf, Arctic Ocean: combining bulk stable isotope and fatty acid signatures. Prog. Oceanogr. 120, 79–92.

Daase, M., Søreide, J.E., 2021. Seasonal variability in non-consumptive mortality of Arctic zooplankton. J. Plankton Res. 43 (4), 565–585.

Daase, M., Varpe, Ø., Falk-Petersen, S., 2014. Non-consumptive mortality in copepods: occurrence of *Calanus* spp. carcasses in the Arctic Ocean during winter. J. Plankton Res. 36 (1), 129–144.

Dalsgaard, J., John, M.S., Kattner, G., Müller-Navarra, D., Hagen, W., 2003. Fatty Acid Trophic Markers in the Pelagic Marine Environment.

Dixon, P., 2003. VEGAN, a package of R functions for community ecology. J. Veg. Sci. 14 (6), 927–930.

Drazen, J.C., Phleger, C.F., Guest, M.A., Nichols, P.D., 2008. Lipid, sterols and fatty acids of abyssal polychaetes, crustaceans, and a cnidarian from the northeast Pacific Ocean: food web implications. Mar. Ecol. Prog. Ser. 372, 157–167.

Duineveld, G.C., Jeffreys, R.M., Lavaleye, M.S., Davies, A.J., Bergman, M.J., Watmough, T., Witbaard, R., 2012. Spatial and tidal variation in food supply to shallow cold-water coral reefs of the Mingulay Reef complex (Outer Hebrides, Scotland). Mar. Ecol. Prog. Ser. 444, 97–115.

Espinasse, B., Tverberg, V., Kristensen, J.A., Skreslet, S., Eiane, K., 2018. Winter mortality in *Calanus* populations in two northern Norwegian fjords from 1984 to 2016. Polar Biol. 41, 1405–1415.

Falk-Petersen, S., Mayzaud, P., Kattner, G., Sargent, J.R., 2009. Lipids and life strategy of Arctic *Calanus*. Mar. Biol. Res. 5 (1), 18–39.

Fisk, A.T., Stern, G.A., Hobson, K.A., Strachan, W.J., Loewen, M.D., Norstrom, R.J., 2001. Persistent organic pollutants (POPs) in a small, herbivorous, Arctic marine zooplankton (*Calanus hyperboreus*): trends from April to July and the influence of lipids and trophic transfer. Mar. Pollut. Bull. 43 (1-6), 93–101.

Fortune, S.M., Ferguson, S.H., Trites, A.W., Hudson, J.M., Baumgartner, M.F., 2020. Bowhead whales use two foraging strategies in response to fine-scale differences in zooplankton vertical distribution. Sci. Rep. 10 (1), 20249.

Franco-Cisterna, B., Stief, P., Glud, R.N., 2021. Temperature effects on carbon mineralization of sinking copepod carcasses. Mar. Ecol. Prog. Ser. 679, 31–45.

Gislason, A., Eiane, K., Reynisson, P., 2007. Vertical distribution and mortality of *Calanus finmarchicus* during overwintering in oceanic waters southwest of Iceland. Mar. Biol. 150, 1253–1263.

Gontikaki, E., Mayor, D.J., Narayanaswamy, B.E., Witte, U., 2011. Feeding strategies of deep-sea sub-Arctic macrofauna of the Faroe-Shetland Channel: combining natural stable isotopes and enrichment techniques. Deep Sea Res. Oceanogr. Res. Pap. 58 (2), 160–172.

Graeve, M., Kattner, G., Piepenburg, D., 1997. Lipids in Arctic benthos: does the fatty acid and alcohol composition reflect feeding and trophic interactions? Polar Biol. 18, 53–61.

Hagen, W., Kattner, G., Graeve, M., 1993. *Calanoides acutus* and *Calanus propinquus*, Antarctic copepods with different lipid storage modes via wax esters or triacylglycerols. Mar. Ecol. Prog. Ser. 135–142.

Halfter, S., Cavan, E.L., Butterworth, P., Swadling, K.M., Boyd, P.W., 2022. "Sinking dead"—how zooplankton carcasses contribute to particulate organic carbon flux in the subantarctic Southern Ocean. Limnol. Oceanogr. 67 (1), 13–25.

Hallanger, I.G., Ruus, A., Warner, N.A., Herzke, D., Evenset, A., Schøyen, M., Gabrielsen, G.W., Borgå, K., 2011. Differences between Arctic and Atlantic fjord systems on bioaccumulation of persistent organic pollutants in zooplankton from Svalbard. Sci. Total Environ. 409 (14), 2783–2795.

Hannides, C.C., Popp, B.N., Landry, M.R., Graham, B.S., 2009. Quantification of zooplankton trophic position in the North Pacific Subtropical Gyre using stable nitrogen isotopes. Limnol. Oceanogr. 54 (1), 50–61.

Hansen, B.H., Tarrant, A.M., Lenz, P.H., Roncalli, V., Almeda, R., Broch, O.J., Altin, D., Tollefsen, K.E., 2024. Effects of petrogenic pollutants on North Atlantic and Arctic *Calanus* copepods: from molecular mechanisms to population impacts. Aquat. Toxicol. 267, 106825.

Hargrave, B.T., Phillips, G.A., Vass, W.P., Bruecker, P., Welch, H.E., Siferd, T.D., 2000. Seasonality in bioaccumulation of organochlorines in lower trophic level arctic marine biota. Environ. Sci. Technol. 34 (6), 980–987.

Harvey, H.R., Eglinton, G., O'Hara, S.C., Corner, E.D., 1987. Biotransformation and assimilation of dietary lipids by *Calanus* feeding on a dinoflagellate. Geochem. Cosmochim. Acta 51 (11), 3031–3040.

Heath, M., Rasmussen, J., Ahmed, Y., Allen, J., Anderson, C., Brierley, A., Brown, L., Bunker, A., Cook, K., Davidson, R., 2008. Spatial demography of *Calanus finmarchicus* in the Irminger Sea. Prog. Oceanogr. 76 (1), 39–88.

Hirche, H.-J., Muyakshin, S., Klages, M., Auel, H., 2006. Aggregation of the Arctic copepod *Calanus hyperboreus* over the ocean floor of the Greenland Sea. Deep Sea Res. Oceanogr. Res. Pap. 53 (2), 310–320.

Hop, H., Falk-Petersen, S., Svendsen, H., Kwasniewski, S., Pavlov, V., Pavlova, O., Søreide, J.E., 2006. Physical and biological characteristics of the pelagic system across Fram Strait to Kongsfjorden. Prog. Oceanogr. 71 (2-4), 182–231.

Howell, K.L., Pond, D.W., Billett, D.S., Tyler, P.A., 2003. Feeding ecology of deep-sea seastars (Echinodermata: Asteroidea): a fatty-acid biomarker approach. Mar. Ecol. Prog. Ser. 255, 193–206.

Hudson, I.R., Pond, D.W., Billett, D.S., Tyler, P.A., Lampitt, R.S., Wolff, G.A., 2004. Temporal variations in fatty acid composition of deep-sea holothurians: evidence of bentho-pelagic coupling. Mar. Ecol. Prog. Ser. 281, 109–120.

Iken, K., Bluhm, B., Gradinger, R., 2005. Food web structure in the high Arctic Canada Basin: evidence from δ 13 C and δ 15 N analysis. Polar Biol. 28, 238–249.

Ingvarsdóttir, A., Houlihan, D.F., Heath, M.R., Hay, S.J., 1999. Seasonal changes in respiration rates of copepodite stage V *Calanus finmarchicus* (Gunnerus). Fish. Oceanogr. 8, 73–83.

Jónasdóttir, S.H., Visser, A.W., Richardson, K., Heath, M.R., 2015. Seasonal copepod lipid pump promotes carbon sequestration in the deep North Atlantic. Proc. Natl. Acad. Sci. 112 (39), 12122–12126.

Jónasdóttir, S.H., Wilson, R.J., Gislason, A., Heath, M.R., 2019. Lipid content in overwintering *Calanus finmarchicus* across the subpolar eastern North Atlantic Ocean. Limnol. Oceanogr. 64 (5), 2029–2043.

Karnovsky, N.J., Kwaśniewski, S., Węsławski, J.M., Walkusz, W., Beszczyńska-Möller, A., 2003. Foraging behavior of little auks in a heterogeneous environment. Mar. Ecol. Prog. Ser. 253, 289–303.

Käß, M., Chikina, M., Vedenin, A., Pineda-Metz, S.E., Soltwedel, T., 2021. Traits and drivers: functioning of macrobenthic communities across the deep Fram Strait (Arctic Ocean). Ecol. Indic. 123, 107324.

Käß, M., Vedenin, A., Hasemann, C., Brandt, A., Soltwedel, T., 2019. Community structure of macrofauna in the deep Fram Strait: a comparison between two bathymetric gradients in ice-covered and ice-free areas. Deep Sea Res. Oceanogr. Res. Pap. 152, 103102.

Kelly, J.R., Scheibling, R.E., 2012. Fatty acids as dietary tracers in benthic food webs. Mar. Ecol. Prog. Ser. 446, 1–22.
Kosobokova, K., Hirche, H.-J., Scherzinger, T., 2002. Feeding ecology of *Spinocalanus antarcticus*, a mesopelagic copepod with a looped gut. Mar. Biol. 141, 503–511.
Kvile, K.Ø., Ashjian, C., Ji, R., 2019. Pan-Arctic depth distribution of diapausing *Calanus* copepods. Biol. Bull. 237 (2), 76–89.
Laakmann, S., Kochzius, M., Auel, H., 2009. Ecological niches of Arctic deep-sea copepods: vertical partitioning, dietary preferences and different trophic levels minimize inter-specific competition. Deep Sea Res. Oceanogr. Res. Pap. 56 (5), 741–756.
Lacey, N.C., Mayor, D.J., Linley, T.D., Jamieson, A.J., 2018. Population structure of the hadal amphipod *Bathycallisoma* (*Scopelocheirus) schellenbergi* in the Kermadec Trench and New Hebrides Trench, SW Pacific. Deep Sea Res. Part II Top. Stud. Oceanogr. 155, 50–60.
Lalande, C., Nöthig, E.-M., Bauerfeind, E., Hardge, K., Beszczynska-Möller, A., Fahl, K., 2016. Lateral supply and downward export of particulate matter from upper waters to the seafloor in the deep eastern Fram Strait. Deep Sea Res. Oceanogr. Res. Pap. 114, 78–89.
Lee, R.F., Hagen, W., Kattner, G., 2006. Lipid storage in marine zooplankton. Mar. Ecol. Prog. Ser. 307, 273–306.
Legeżyńska, J., 2008. Food resource partitioning among Arctic sublittoral lysianassoid amphipods in summer. Polar Biol. 31 (6), 663–670.
Legeżyńska, J., Kędra, M., Walkusz, W., 2012. When season does not matter: summer and winter trophic ecology of Arctic amphipods. Hydrobiologia 684, 189–214.
Lehtiniemi, M., Viitasalo, M., Kuosa, H., 2002. 'Diet composition influences the growth of the pelagic mysid shrimp, Mysis mixta (Mysidacea)'. Boreal Environ. Res. 7 (2), 121.
Lörz, A.-N., Nack, M., Tandberg, A.H.S., Brix, S., Schwentner, M., 2024. 'A New deep-sea Species of Halirages Boeck, 1871 (Crustacea: Amphipoda: Calliopiidae) Inhabiting Sponges'.
Maar, K., Papadimitraki, M., Ruiz, L.H., Broughton, R., Jónasdóttir, S.H., 2023. Lipids in meso-and bathypelagic fishes from the North Atlantic Ocean: dietary inputs suggested from fatty acid trophic markers. Mar. Ecol. Prog. Ser. 717, 127–141.
Mayor, D.J., Cook, K., Thornton, B., Walsham, P., Witte, U.F., Zuur, A.F., Anderson, T.R., 2011. Absorption efficiencies and basal turnover of C, N and fatty acids in a marine Calanoid copepod. Funct. Ecol. 25 (3), 509–518.
Mayor, D.J., Cook, K.B., Anderson, T.R., Belcher, A., Jenkins, H., Lindeque, P., Tarling, G. A., Pond, D., 2020a. Marine Copepods, the wildebeest of the ocean. Frontiers for Young Minds 8 (18).
Mayor, D.J., Cook, K.B., Thornton, B., Atherden, F., Tarling, G.A., Anderson, T.R., 2022. Biomass turnover rates in metabolically active and inactive marine calanoid copepods. Front. Mar. Sci. 9, 907290.
Mayor, D.J., Gentleman, W.C., Anderson, T.R., 2020b. Ocean carbon sequestration: particle fragmentation by copepods as a significant unrecognised factor? Explicitly representing the role of copepods in biogeochemical models may fundamentally improve understanding of future ocean carbon storage. Bioessays 42 (12), 2000149.
Mayor, D.J., Sanders, R., Giering, S.L., Anderson, T.R., 2014. Microbial gardening in the ocean's twilight zone: detritivorous metazoans benefit from fragmenting, rather than ingesting, sinking detritus: fragmentation of refractory detritus by zooplankton beneath the euphotic zone stimulates the harvestable production of labile and nutritious microbial biomass. Bioessays 36 (12), 1132–1137.
Mayor, D.J., Sharples, C.J., Webster, L., Walsham, P., Lacaze, J.-P., Cousins, N.J., 2013. Tissue and size-related changes in the fatty acid and stable isotope signatures of the deep sea grenadier fish *Coryphaenoides armatus* from the Charlie-Gibbs Fracture Zone region of the Mid-Atlantic Ridge. Deep Sea Res. Part II Top. Stud. Oceanogr. 98, 421–430.
Mayor, D.J., Zuur, A.F., Solan, M., Paton, G.I., Killham, K., 2010. Factors affecting benthic impacts at Scottish fish farms. Environ. Sci. Technol. 44 (6), 2079–2084.
McGovern, M., Berge, J., Szymczycha, B., Węsławski, J.M., Renaud, P.E., 2018. Hyperbenthic food-web structure in an Arctic fjord. Mar. Ecol. Prog. Ser. 603, 29–46.
Neto, R.R., Wolff, G.A., Billett, D.S., Mackenzie, K.L., Thompson, A., 2006. The influence of changing food supply on the lipid biochemistry of deep-sea holothurians. Deep Sea Res. Oceanogr. Res. Pap. 53 (3), 516–527.
Nöthig, E.-M., Bracher, A., Engel, A., Metfies, K., Niehoff, B., Peeken, I., Bauerfeind, E., Cherkasheva, A., Gäbler-Schwarz, S., Hardge, K., 2015. Summertime plankton ecology in Fram Strait—A compilation of long-and short-term observations. Polar Res. 34 (1), 23349.
Nöthig, E.-M., Ramondenc, S., Haas, A., Hehemann, L., Walter, A., Bracher, A., Lalande, C., Metfies, K., Peeken, I., Bauerfeind, E., 2020. Summertime chlorophyll a and particulate organic carbon standing stocks in surface waters of the Fram Strait and the Arctic Ocean (1991–2015). Front. Mar. Sci. 7, 350.
Oliveira, A.F., Marques, S.C., Pereira, J.L., Azeiteiro, U.M., 2023. A review of the order mysida in marine ecosystems: what we know what is yet to be known. Mar. Environ. Res. 188, 106019.
Parzanini, C., Parrish, C.C., Hamel, J.-F., Mercier, A., 2018. Trophic relationships of deep-sea benthic invertebrates on a continental margin in the NW Atlantic inferred by stable isotope, elemental, and fatty acid composition. Prog. Oceanogr. 168, 279–295.
Pearson, M., Gage, J., 1984. Diets of some deep-sea brittle stars in the Rockall Trough. Mar. Biol. 82, 247–258.
Pinti, J., Jónasdóttir, S.H., Record, N.R., Visser, A.W., 2023. The global contribution of seasonally migrating copepods to the biological carbon pump. Limnol. Oceanogr. 68 (5), 1147–1160.
Pond, D.W., 2012. The physical properties of lipids and their role in controlling the distribution of zooplankton in the oceans. J. Plankton Res. 34 (6), 443–453.
Pond, D.W., Tarling, G.A., Ward, P., Mayor, D.J., 2012. Wax ester composition influences the diapause patterns in the copepod *Calanoides* acutus. Deep Sea Res. Part II Top. Stud. Oceanogr. 59, 93–104.
Pouch, A., Zaborska, A., 2015. Climate change influence on migration of contaminants in the Arctic marine environment. Impact of climate changes on marine environments 75–90.
Richoux, N.B., Deibel, D., Thompson, R.J., Parrish, C.C., 2005. Seasonal and developmental variation in the fatty acid composition of *Mysis mixta* (Mysidacea) and *Acanthostepheia malmgreni* (Amphipoda) from the hyperbenthos of a cold-ocean environment (Conception Bay, Newfoundland). J. Plankton Res. 27 (8), 719–733.
Ritterhoff, J., Zauke, G.-P., 1997. Trace metals in field samples of zooplankton from the Fram Strait and the Greenland Sea. Sci. Total Environ. 199 (3), 255–270.
Sainte-Marie, B., 1992. Foraging of scavenging deep-sea lysianassoid amphipods. Deep-Sea Food Chains and the Global Carbon Cycle. Springer, pp. 105–124.
Sainte-Marie, B., Brunel, P., 1985. Suprabenthic gradients of swimming activity by cold-water gammaridean amphipod Crustacea over a muddy shelf in the Gulf of Saint Lawrence. Mar. Ecol. Prog. Ser. 57–69.
Sargent, J., Falk-Petersen, S., 1988. The Lipid Biochemistry of Calanoid Copepods. Hydrobiologia 167 (1), 104–114.
Sargent, J., Gatten, R., McIntosh, R., 1977. Wax esters in the marine environment—their occurrence, formation, transformation and ultimate fates. Mar. Chem. 5 (4-6), 573–584.
Savineau, E.L.-R., Cook, K.B., Blackbird, S.J., Stowasser, G., Kiriakoulakis, K., Preece, C., Fielding, S., Belcher, A.C., Wolff, G.A., Tarling, G.A., 2024. Investigating the physiological ecology of mesopelagic zooplankton in the Scotia sea (Southern ocean) using lipid and stable isotope signatures. Deep Sea Res. Oceanogr. Res. Pap. 208, 104317.
Schmidt, K., Niehoff, B., Cornils, A., Hagen, W., Flores, H., Heuzé, C., Welteke, N., Knüppel, N., Dorschner, S., Woll, M., 2025. Seasonal vertical migration of large polar copepods reinterpreted as a dispersal mechanism throughout the water column. Commun. Earth Environ. 6 (1), 1–18.
Schmittmann, L., Schindler, S.V., Bayer, T., Fuss, J., Havermans, C., Merten, V., Hoving, H.J.T., 2024. The sinking Dead—Arctic Deep-Sea scavengers' diet suggests Nekton as vector in benthopelagic coupling. Environmental DNA 6 (5), e70020.
Scott, C.L., Kwasniewski, S., Falk-Petersen, S., Sargent, J.R., 2002. Species differences, origins and functions of fatty alcohols and fatty acids in the wax esters and phospholipids of *Calanus hyperboreus, C. glacialis* and *C. finmarchicus* from Arctic waters. Mar. Ecol. Prog. Ser. 235, 127–134.
Soltwedel, T., Bauerfeind, E., Bergmann, M., Bracher, A., Budaeva, N., Busch, K., Cherkasheva, A., Fahl, K., Grzelak, K., Hasemann, C., 2016. Natural variability or anthropogenically-induced variation? Insights from 15 years of multidisciplinary observations at the arctic marine LTER site HAUSGARTEN. Ecol. Indic. 65, 89–102.
Soltwedel, T., Jaeckisch, N., Ritter, N., Hasemann, C., Bergmann, M., Klages, M., 2009. Bathymetric patterns of megafaunal assemblages from the arctic deep-sea observatory HAUSGARTEN. Deep Sea Res. Oceanogr. Res. Pap. 56 (10), 1856–1872.
Soltwedel, T., von Juterzenka, K., Premke, K., Klages, M., 2003. What a lucky shot! photographic evidence for a medium-sized natural food-fall at the deep seafloor. Oceanol. Acta 26 (5-6), 623–628.
Soltwedel, T., 2025. LTER Observatory HAUSGARTEN, DEIMS-SDR. https://deims.org/f6d9ed12-6bc1-47fb-8e81-ef24e9579596 (accessed 30 April 2025).
Søreide, J.E., Carroll, M.L., Hop, H., Ambrose Jr, W.G., Hegseth, E.N., Falk-Petersen, S., 2013. Sympagic-pelagic-benthic coupling in Arctic and Atlantic waters around Svalbard revealed by stable isotopic and fatty acid tracers. Mar. Biol. Res. 9 (9), 831–850.
Søreide, J.E., Falk-Petersen, S., Hegseth, E.N., Hop, H., Carroll, M.L., Hobson, K.A., Blachowiak-Samolyk, K., 2008. Seasonal feeding strategies of *Calanus* in the high-Arctic Svalbard region. Deep Sea Res. Part II Top. Stud. Oceanogr. 55 (20-21), 2225–2244.
Suhr, S.B., Pond, D.W., Gooday, A.J., Smith, C.R., 2003. Selective feeding by benthic Foraminifera on phytodetritus on the western Antarctic Peninsula shelf: evidence from fatty acid biomarker analysis. Mar. Ecol. Prog. Ser. 262, 153–162.
Tamelander, T., Søreide, J.E., Hop, H., Carroll, M.L., 2006. Fractionation of stable isotopes in the Arctic marine copepod *Calanus glacialis*: effects on the isotopic composition of marine particulate organic matter. J. Exp. Mar. Biol. Ecol. 333 (2), 231–240.
Tarling, G.A., Belcher, A., Blackwell, M., Castellani, C., Cook, K.B., Cottier, F.R., Dewar-Fowler, V., Freer, J.J., Gerrish, L., Johnson, M.L., 2022a. Carbon and lipid contents of the copepod *Calanus finmarchicus* entering diapause in the Fram Strait and their contribution to the boreal and Arctic lipid pump. Front. Mar. Sci. 9, 926462.

Tarling, G.A., Freer, J.J., Banas, N.S., Belcher, A., Blackwell, M., Castellani, C., Cook, K. B., Cottier, F.R., Daase, M., Johnson, M.L., 2022b. Can a key boreal *Calanus* copepod species now complete its life-cycle in the Arctic? Evidence and implications for Arctic food-webs. Ambio 51 (2), 333–344.

Turner, J.T., 2015. Zooplankton fecal pellets, marine snow, phytodetritus and the ocean's biological pump. Prog. Oceanogr. 130, 205–248.

Varpe, Ø., Fiksen, Ø., Slotte, A., 2005. Meta-ecosystems and biological energy transport from ocean to coast: the ecological importance of herring migration. Oecologia 146, 443–451.

Viherluoto, M., Viitasalo, M., 2001. Temporal variability in functional responses and prey selectivity of the pelagic mysid, *Mysis mixta*, in natural prey assemblages. Mar. Biol. 138, 575–583.

Visser, A.W., Grønning, J., Jónasdóttir, S.H., 2017. *Calanus hyperboreus* and the lipid pump. Limnol. Oceanogr. 62 (3), 1155–1165.

Wexels Riser, C., Reigstad, M., Wassmann, P., Arashkevich, E., Falk-Petersen, S., 2007. Export or retention? Copepod abundance, faecal pellet production and vertical flux in the marginal ice zone through snap shots from the northern Barents Sea. Polar Biol. 30, 719–730.

Wiedmann, I., Ershova, E., Bluhm, B.A., Nöthig, E.-M., Gradinger, R.R., Kosobokova, K., Boetius, A., 2020. What feeds the benthos in the Arctic Basins? Assembling a carbon budget for the deep Arctic Ocean. Front. Mar. Sci. 7, 224.

Yamamuro, M., Kayanne, H., 1995. Rapid direct determination of organic carbon and nitrogen in carbonate-bearing sediments with a Yanaco MT-5 CHN analyzer. Limnol. Oceanogr. 40 (5), 1001–1005.